15 mg/kg 60 min before NMDA injection markedly reduced TUNEL-positive cells. Results of cell count in GCL and INL of three to four independent experiments are shown in Fig. 4.

3.3. Effect of MEK inhibitor on anti-apoptotic effect of ATRA in the rat retina

To examine whether the activation of ERK is involved in the anti-apoptotic effect of ATRA, we co-administrated with U0126, a MEK inhibitor and ATRA. As shown in Fig. 5, TUNEL-positive cells were observed in the GCL and in the inner side of the INL, but not in the ONL, in the retina of the animals treated both U0126 (1 nmol, 15 min before ATRA treatment) and ATRA (15 mg/kg, 60 min before NMDA injection). U0126 (1 nmol) itself did not affect the apoptosis induced by intravitreous NMDA injection. U0126 (2 nmol) itself reduced the number of TUNEL-positive cells in GCL, whereas the concentration of U0126 tended to block the protective effects of ATRA in INL. Results of cell count in GCL and INL of three to four independent experiments are shown in Fig. 6.

4. Discussion

In the present study, we demonstrated that ATRA has a protective effect on NMDA-induced neuron damage and an anti-apoptotic effect in the rat retina *in vivo*. The dose of ATRA which showed the protective effects in the present study (15 mg/kg for the first two days and 10 mg/kg for the following five days) has been shown to have anti-inflammatory properties in an experimental rat models of nephropathy (Moreno-Manzano et al., 2003), to enhance nociceptive withdrawal reflexes in rats (Romero-Sandoval et al., 2004), and also to induce an increase in the prostaglandin E2 concentration in rat plasma and liver homogenate (Devaux et al., 2001), and the doses were also well below the toxic doses reported in the similar species (Teelmann, 1989). In addition, no protective effect was seen in some animals treated with the highest dose of ATRA in the present study. Although the reason why the highest dose did not induce protective effects could not be clarified in the present study, it is possible that some pro-apoptotic signals may be activated simultaneously by the dose of ATRA. Because the dose of ATRA itself did not affect retinal morphology, toxicity of ATRA is much less likely to be involved in the underlying mechanism. We propose that the middle dose of ATRA in the present study (15 mg/kg for the first two days and 10 mg/kg for the following five days) is the best to bring its beneficial effects in our experimental model and maybe also in other experimental models using the rats.

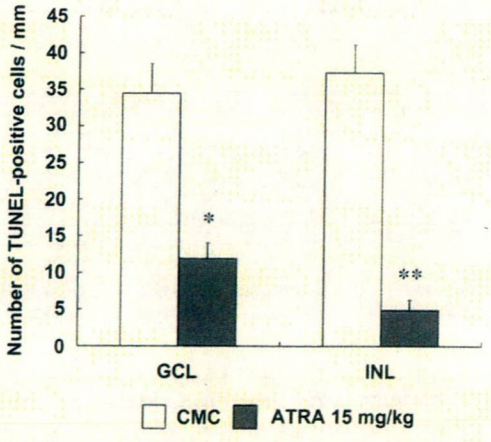

Fig. 4. The result of TUNEL-positive cell count. TUNEL staining was examined 6 h after NMDA injection. The number of TUNEL-positive cells was counted manually at 1.0 mm from the center of the optic disk using a microscope: GCL (ganglion cell layer); INL (inner nuclear layer). The data represent the means ± S.E.M. of four rats per group. $^{*}P<0.05$, $^{**}P<0.01$ vs. CMC-treated group.

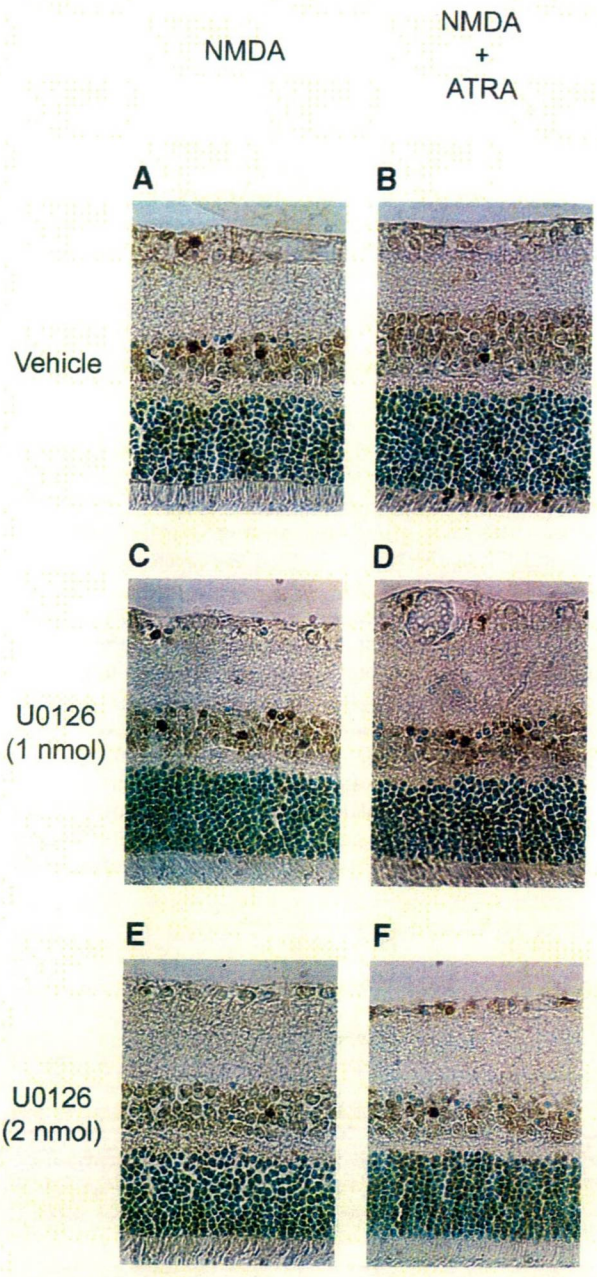

Fig. 5. Representative photomicrographs showing the effect of U0126, an extracellular signal-regulated kinase/mitogen-activated protein kinase kinase (MEK) inhibitor, on anti-apoptotic action of ATRA. TUNEL-positive nuclei are shown in the ganglion cell layer and the inner nuclear layer of CMC (the vehicle of ATRA)-treated and NMDA and the vehicle of U0126-injected retinae ($n=5$) (A). In the retina treated with 15 mg/kg ATRA 60 min before NMDA and the vehicle of U0126 injection, the number of the positive nuclei is smaller than that in the CMC and NMDA-treated retinae ($n=3$) (B). TUNEL-positive nuclei are shown in the ganglion cell layer and the inner nuclear layer of CMC-treated and the vehicle of NMDA and U0126-injected retinae ($n=5$) (C). In the retina treated with 15 mg/kg ATRA 60 min before NMDA and 1 nmol/eye U0126 injection, the number of the positive nuclei is larger than that in the ATRA and NMDA-treated retinae ($n=5$) (D). In the retina injected 2 nmol/eye U0126 injection, the numbers of TUNEL-positive cells were reduced with (F; $n=6$) or without (E; $n=3$) treatment with ATRA. Scale bar = 50 μm. Original magnification is ×200.

Retinoic acid has not only genomic effects, such as induction of various genes, but also rapid non-genomic effects on cytoplasmic messenger pathways. In the present study, we found that oral administration of ATRA 60 min before NMDA injection led to the

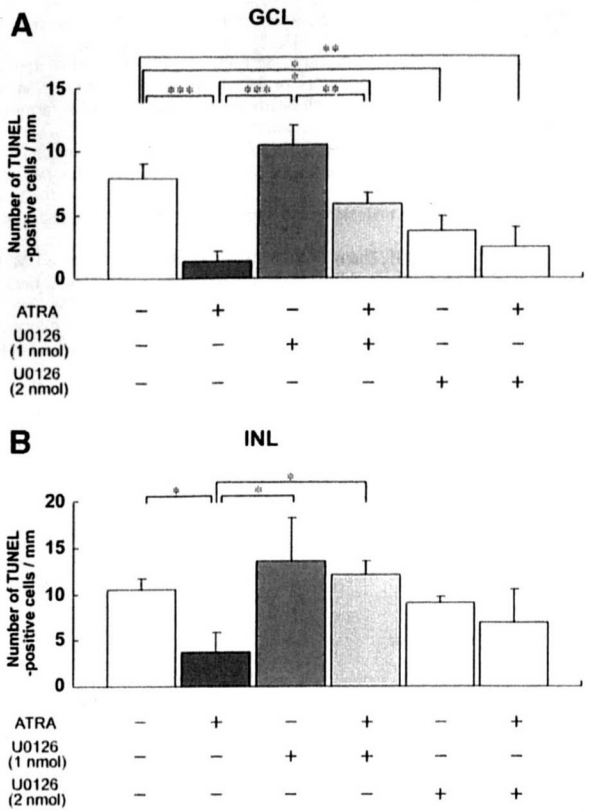

Fig. 6. The result of TUNEL-positive cell count in the experiments using U0126. TUNEL staining was examined 6 h after NMDA injection. The number of TUNEL-positive cells was counted manually at 1.0 mm from the center of the optic disk using a microscope: GCL (ganglion cell layer); INL (inner nuclear layer). The data represent the means ± S.E.M. of three to five rats per group. $^{*}P<0.05$, $^{**}P<0.01$, $^{***}P<0.001$ between the indicated groups.

neuroprotection in retina. The anti-apoptotic effect of ATRA is unlikely to be mediated by the genomic action of its nuclear receptors, because it usually takes at least a few hours. In addition, the anti-apoptotic effect was inhibited by 1 nmol/eye U0126, a MEK inhibitor. Because 2 nmol/eye U0126 itself reduced apoptosis induced by NMDA in GCL, it is possible that the dose of U0126 nonselectively inhibited pro-apoptotic kinases, such as JNK and p38 MAP kinase in GCL. The results in the present study also suggest that 1 nmol/eye is the best dose to block ERK in our experimental system. To strengthen the involvement of MEK in ATRA-induced protection, we tried to see the effects of U0126 on the histological protection by ATRA 7 days after NMDA injection, and the effects of PD098059, another MEK inhibitor. Unfortunately, we gave these experiments up, because of the damage of eyeballs induced by repetitive intravitreous injection, and anti-apoptotic effects of its vehicle, respectively. ATRA is known to activate neuronal ERK through retinoic acid receptors and/or retinoid X receptors in a non-genomic manner (Canon et al., 2004). ATRA has also been shown to inhibit the dephosphorylation of ERK in the oxygen–glucose-deprived rat cultured hippocampus slice (Shinozaki et al., 2007). To combine our results and previous reports, it is possible that ATRA activates ERK *via* its non-genomic action, leading to the protection of retinal neurons from NMDA-induced apoptosis.

ATRA is known to induce the expression of mitogen-activated protein kinase phosphatase-1 (MKP-1), which protects mesangial cells against hydrogen peroxide-induced cell death by dephosphorylation of JNK and p38 MAP kinase (Konta et al., 2001). MKP-1 has been reported to dephosphorylate JNK and p38 MAP kinase, but not ERK (Wu and Bennett, 2005). In the previous study, ATRA has been shown to inhibit the activation of JNK and p38 MAP kinase, which are pro-apoptotic signals in the oxygen–glucose-deprived rat cultured hippocampus slice (Shinozaki et al., 2007). Therefore, it is of interest to examine whether the inhibition of JNK and p38 by ATRA also plays a significant role in its cytoprotective effect in the retina. To clarify this point, further progress of the reagents that selectively activate JNK and/or p38 MAP kinase, and experiments using such reagents are needed.

In conclusion, the present study indicates that ATRA has a protective effect on retinal neurons against NMDA-induced apoptosis *in vivo*. The activation of ERK is possible to be involved in the underlying mechanisms. ATRA easily passes through the blood–brain barrier and reach the central nervous system (Crandall et al., 2004). Because of its lipophilic nature, orally administered ATRA presumably passes through the blood-retinal barrier relatively easily. Our findings suggest that ATRA may be effective for treatment of retinal diseases known to be associated with glutamate excitotoxicity such as retinal vessel occlusion and glaucoma.

Acknowledgments

This work is supported by the Japanese Ministry of Education, Science, Sports and Culture, Grant-in-Aid for Young Scientists (B) #17790174 (KS), and grants from the Japanese Ministry of Health, Labor and Welfare and the Japan Health Sciences Foundation #KHC1014 (YS).

References

Ahlemeyer, B., Krieglstein, J., 1998. Retinoic acid reduces staurosporine-induced apoptotic damage in chick embryonic neurons by suppressing reactive oxygen species production. Neurosci. Lett. 246, 93–96.
Canon, E., Cosgaya, J.M., Scsucova, S., Aranda, A., 2004. Rapid effects of retinoic acid on CREB and ERK phosphorylation in neuronal cells. Mol. Biol. Cell 15, 5583–5592.
Chambon, P., 1994. The retinoid signaling pathway: molecular and genetic analyses. Semin. Cell Biol. 5, 115–125.
Chambon, P., 1996. A decade of molecular biology of retinoic acid receptors. FASEB J. 10, 940–954.
Choi, D.W., 1987. Ionic dependence of glutamate neurotoxicity in cortical cell culture. J. Neurosci. 7, 369–379.
Choi, D.W., 1988. Calcium-mediated neurotoxicity: relationship to specific channel types and role in ischemic damage. Trends Neurosci. 11, 465–469.
Crandall, J., Sakai, Y., Zhang, J., Koul, O., Mineur, Y., Crusio, W.E., McCaffery, P., 2004. 13-Cis-retinoic acid suppresses hippocampal cell division and hippocampal-dependent learning in mice. Proc. Natl. Acad. Sci. U. S. A. 101, 5111–5116.
David, P., Lusky, M., Teichberg, V.I., 1988. Involvement of excitatory neurotransmitters in the damage produced in chick embryo retinas by anoxia and extracellular high potassium. Exp. Eye Res. 46, 657–662.
Devaux, Y., Seguin, C., Grosjean, S., de Talancé, N., Schwartz, M., Burlet, A., Zannad, F., Meistelman, C., Mertes, P.M., Ungureanu-Longrois, D., 2001. Retinoic acid and lipopolysaccharide act synergistically to increase prostanoid concentrations in rats in vivo. J. Nutr. 131, 2628–2635.
Han, B.H., Holtzman, D.M., 2000. BDNF protects the neonatal brain from hypoxic–ischemic injury in vivo via the ERK pathway. J. Neurosci. 20, 5775–5781.
Hetman, M., Kanning, K., Cavanaugh, J.E., Xia, Z., 1999. Neuroprotection by brain-derived neurotrophic factor is mediated by extracellular signal-regulated kinase and phosphatidylinositol 3-kinase. J. Biol. Chem. 274, 22569–22580.
Kilic, E., Kilic, U., Soliz, J., Bassetti, C.L., Gassmann, M., Hermann, D.M., 2005. Brain-derived erythropoietin protects from focal cerebral ischemia by dual activation of ERK-1/-2 and Akt pathways. FASEB J. 19, 2026–2028.
Konta, T., Xu, Q., Furusu, A., Nakayama, K., Kitamura, M., 2001. Selective roles of retinoic acid receptor and retinoid x receptor in the suppression of apoptosis by all-trans-retinoic acid. J. Biol. Chem. 276, 12697–12701.
Kuehn, M.H., Fingert, J.H., Kwon, Y.H., 2005. Retinal ganglion cell death in glaucoma: mechanisms and neuroprotective strategies. Ophthalmol. Clin. North Am. 18, 383–395.
LaVail, M.M., Battelle, B.A., 1975. Influence of eye pigmentation and light deprivation on inherited retinal dystrophy in the rat. Exp. Eye Res. 21, 167–192.
Louzada-Júnior, P., Dias, J.J., Santos, W.F., Lachat, J.J., Bradford, H.F., Coutinho-Netto, J., 1992. Glutamate release in experimental ischaemia of the retina: an approach using microdialysis. J. Neurochem. 59, 358–363.
Maden, M., 2001. Role and distribution of retinoic acid during CNS development. Int. Rev. Cytol. 209, 1–77.
Moreno-Manzano, V., Mampaso, F., Sepúlveda-Muñoz, J.C., Alique, M., Chen, S., Ziyadeh, F.N., Iglesias-de la Cruz, M.C., Rodríguez, J., Nieto, E., Orellana, J.M., Reyes, P., Arribas, I., Xu, Q., Kitamura, M., Lucio Cazana, F.J., 2003. Retinoids as a potential treatment for experimental puromycin-induced nephrosis. Br. J. Pharmacol. 139, 823–831.
Palczewski, K., Kumasaka, T., Hori, T., Behnke, C.A., Motoshima, H., Fox, B.A., Le Trong, I., Teller, D.C., Okada, T., Stenkamp, R.E., Yamamoto, M., Miyano, M., 2000. Crystal structure of rhodopsin: a G protein-coupled receptor. Science 289, 739–745.
Pasquali, D., Chieffi, P., Deery, W.J., Nicoletti, G., Bellastella, A., Sinisi, A.A., 2005. Differential effects of all-trans-retinoic acid (RA) on Erk1/2 phosphorylation and

cAMP accumulation in normal and malignant human prostate epithelial cells: Erk1/2 inhibition restores RA-induced decrease of cell growth in malignant prostate cells. Eur. J. Endocrinol. 152, 663–669.
Romero-Sandoval, E.A., Alique, M., Moreno-Manzano, V., Molina, C., Lucio, F.J., Herrero, J.F., 2004. The oral administration of retinoic acid enhances nociceptive withdrawal reflexes in rats with soft-tissue inflammation. Inflamm. Res. 53, 297–303.
Rössler, O.G., Giehl, K.M., Thiel, G., 2004. Neuroprotection of immortalized hippocampal neurons by brain-derived neurotrophic factor and Raf-1 protein kinase: role of extracellular signal-regulated protein kinase and phosphatidylinositol 3-kinase. J. Neurochem. 88, 1240–1252.
Roth, S., Li, B., Rosenbaum, P.S., Gupta, H., Goldstein, I.M., Maxwell, K.M., Gidday, J.M., 1998. Preconditioning provides complete protection against retinal ischemic injury in rats. Invest. Ophthalmol. Vis. Sci. 39, 777–785.
Sahin, M., Karauzum, S.B., Perry, G., Smith, M.A., Aliciguzel, Y., 2005. Retinoic acid isomers protect hippocampal neurons from amyloidbeta induced neurodegeneration. Neurotox. Res. 7, 243–250.
Sakamoto, K., Yonoki, Y., Kubota, Y., Kuwagata, M., Saito, M., Nakahara, T., Ishii, K., 2006. Inducible nitric oxide synthase inhibitors abolished histological protection by late ischemic preconditioning in rat retina. Exp. Eye Res. 82, 512–518.
Sakamoto, K., Kawakami, T., Shimada, M., Yamaguchi, A., Kuwagata, M., Saito, M., Nakahara, T., Ishii, K., 2009. Histological protection by cilnidipine, a dual L/N-type Ca^{2+} channel blocker, against neurotoxicity induced by ischemia–reperfusion in rat retina. Exp. Eye Res. 88, 974–982.
Shinozaki, Y., Sato, Y., Koizumi, S., Ohno, Y., Nagao, T., Inoue, K., 2007. Retinoic acids acting through retinoid receptors protect hippocampal neurons from oxygen-glucose deprivation-mediated cell death by inhibition of c-jun-N-terminal kinase and p38 mitogen-activated protein kinase. Neuroscience 147, 153–163.
Siliprandi, R., Canella, R., Carmignoto, G., Schiavo, N., Zanellato, A., Zanoni, R., Vantini, G., 1992. N-methyl-D-aspartate-induced neurotoxicity in the adult rat retina. Vis. Neurosci. 8, 567–573.
Teelmann, K., 1989. Retinoids: toxicology and teratogenicity to date. Pharmacol. Ther. 40, 29–43.
Toriu, N., Akaike, A., Yasuyoshi, H., Zhang, S., Kashii, S., Honda, Y., Shimazawa, M., Hara, H., 2000. Lomerizine, a Ca^{2+} channel blocker, reduces glutamate-induced neurotoxicity and ischemia/reperfusion damage in rat retina. Exp. Eye Res. 70, 475–484.
Unoki, K., LaVail, M.M., 1994. Protection of the rat retina from ischemic injury by brain-derived neurotrophic factor, ciliary neurotrophic factor, and basic fibroblast growth factor. Invest. Ophthalmol. Vis. Sci. 35, 907–915.
Wu, J.J., Bennett, A.M., 2005. Essential role for mitogen-activated protein (MAP) kinase phosphatase-1 in stress-responsive MAP kinase and cell survival signaling. J. Biol. Chem. 280, 16461–16466.

THE JOURNAL OF BIOLOGICAL CHEMISTRY VOL. 285, NO. 17, pp. 13244–13253, April 23, 2010

Phosphorylation of TRPC6 Channels at Thr^{69} Is Required for Anti-hypertrophic Effects of Phosphodiesterase 5 Inhibition*

Received for publication, October 8, 2009, and in revised form, February 12, 2010 Published, JBC Papers in Press, February 22, 2010, DOI 10.1074/jbc.M109.074104

Motohiro Nishida[‡], Kenta Watanabe[‡], Yoji Sato[§], Michio Nakaya[‡], Naoyuki Kitajima[‡], Tomomi Ide[¶], Ryuji Inoue[‖], and Hitoshi Kurose[‡1]

From the [‡]Department of Pharmacology and Toxicology, Graduate School of Pharmaceutical Sciences, and the [¶]Department of Cardiovascular Medicine, Graduate School of Medical Sciences, Kyushu University, Higashi-ku, Fukuoka 812-8582, the [§]Division of Cellular and Gene Therapy Products, National Institute of Health Sciences, Setagaya, Tokyo 158-8501, and the [‖]Department of Physiology, School of Medicine, Fukuoka University, 7-45-1 Nanakuma, Jyonan-ku, Fukuoka 814-0180, Japan

Activation of Ca^{2+} signaling induced by receptor stimulation and mechanical stress plays a critical role in the development of cardiac hypertrophy. A canonical transient receptor potential protein subfamily member, TRPC6, which is activated by diacylglycerol and mechanical stretch, works as an upstream regulator of the Ca^{2+} signaling pathway. Although activation of protein kinase G (PKG) inhibits TRPC6 channel activity and cardiac hypertrophy, respectively, it is unclear whether PKG suppresses cardiac hypertrophy through inhibition of TRPC6. Here, we show that inhibition of cGMP-selective PDE5 (phosphodiesterase 5) suppresses endothelin-1-, diacylglycerol analog-, and mechanical stretch-induced hypertrophy through inhibition of Ca^{2+} influx in rat neonatal cardiomyocytes. Inhibition of PDE5 suppressed the increase in frequency of Ca^{2+} spikes induced by agonists or mechanical stretch. However, PDE5 inhibition did not suppress the hypertrophic responses induced by high KCl or the activation of protein kinase C, suggesting that PDE5 inhibition suppresses Ca^{2+} influx itself or molecule(s) upstream of Ca^{2+} influx. PKG activated by PDE5 inhibition phosphorylated TRPC6 proteins at Thr^{69} and prevented TRPC6-mediated Ca^{2+} influx. Substitution of Ala for Thr^{69} in TRPC6 abolished the anti-hypertrophic effects of PDE5 inhibition. In addition, chronic PDE5 inhibition by oral sildenafil treatment actually induced TRPC6 phosphorylation in mouse hearts. Knockdown of RGS2 (regulator of G protein signaling 2) and RGS4, both of which are activated by PKG to reduce $G\alpha_q$-mediated signaling, did not affect the suppression of receptor-activated Ca^{2+} influx by PDE5 inhibition. These results suggest that phosphorylation and functional suppression of TRPC6 underlie prevention of pathological hypertrophy by PDE5 inhibition.

Pathological hypertrophy of the heart, induced by pressure overload, such as chronic hypertension and aortic stenosis, is a major risk factor for heart failure and cardiovascular mortality (1). Neurohumoral factors, such as norepinephrine, angiotensin II (Ang II),[2] and endothelin-1 (ET-1), and mechanical stress are believed to be prominent contributors for pressure overload-induced cardiac hypertrophy (2, 3). Neurohumoral factors stimulate G_q protein-coupled receptors, leading to a sustained increase in $[Ca^{2+}]_i$ through activation of phospholipase C. Mechanical stress also increases $[Ca^{2+}]_i$ through Ca^{2+} influx-dependent pathways (4). The increase in $[Ca^{2+}]_i$ induces activation of Ca^{2+}-sensitive effectors, such as Ca^{2+}/calmodulin-dependent serine/threonine phosphatase calcineurin (3, 5), Ca^{2+}/calmodulin-dependent kinase II (6, 7), and calmodulin-binding transcription factor (8), which in turn induces hypertrophic gene expressions. Although the mechanism of Ca^{2+}-mediated hypertrophy is extensively analyzed, it is not fully understood how these Ca^{2+} targets specifically decode the alteration of $[Ca^{2+}]_i$ under the conditions of the rhythmic Ca^{2+} increases required for contraction.

In excitable cardiomyocytes, increases in the frequency or amplitude of Ca^{2+} transients evoked by Ca^{2+} influx-induced Ca^{2+} release have been suggested to encode signals for induction of hypertrophy (9). A partial depolarization of plasma membrane by receptor stimulation is reported to increase the frequency of Ca^{2+} oscillations, leading to activation of nuclear factor of activated T cells (NFAT), a transcription factor that is predominantly regulated by calcineurin (10). Recent reports have indicated that transient receptor potential canonical (TRPC) subfamily proteins play an essential role in agonist-induced membrane depolarization (11, 12). The relevance of TRPC channels to pathological hypertrophy is underscored by the observations that heart-targeted transgenic mice expressing TRPC channels caused hypertrophy (13, 14) and that TRPC proteins were up-regulated in hypertrophied and failing hearts (14–17). Among seven TRPC subfamilies, increased channel activities of TRPC1, TRPC3, and TRPC6 have been implicated in cardiac hypertrophy *in vivo*. TRPC1 is known to function not

* This study was supported by grants from the Ministry of Education, Culture, Sports, Science, and Technology of Japan (to M. Nishida, M. Nakaya, and H. Kurose), a grant-in-aid for scientific research on Innovative Areas (to M. Nishida), a grant-in-aid for scientific research on Priority Areas (H. Kurose), and grants from the Naito Foundation, the Nakatomi Foundation, the Sapporo Bioscience Foundation (M. Nishida), and the Mochida Memorial Foundation for Medical and Pharmaceutical Research (to M. Nakaya).

[1] To whom correspondence should be addressed. Tel./Fax: 81-92-642-6884; E-mail: kurose@phar.kyushu-u.ac.jp.

[2] The abbreviations used are: Ang II, angiotensin II; BNP, brain natriuretic peptide; CA-NFAT, constitutively active NFAT; DAG, diacylglycerol; $DiBAC_4(3)$, bis(1,3-dibutylbarbituric acid)trimethine oxonol; DN-TRPC6, dominant negative TRPC6; ET-1, endothelin-1; BTP2, 4-methyl-4′-[3,5-bis(trifluoromethyl)-1H-pyrazol-1-yl]-1,2,3-thiadiazole-5-carboxanilide; NFAT, nuclear factor of activated T cells; OAG, a DAG derivative, 1-oleoyl-2-acetyl-*sn*-glycerol; TRPC, transient receptor potential canonical; PDE5-I, phosphodiesterase 5-selective inhibitor: 4-[[3′,4′-(methylenedioxy)benzyl]amino]-6-methoxyquinazoline; RGS, regulator of G protein signaling; PKG, protein kinase G; WT, wild type; 8-Br-cGMP, 8-bromo-cyclic GMP; siRNA, small interfering RNA.

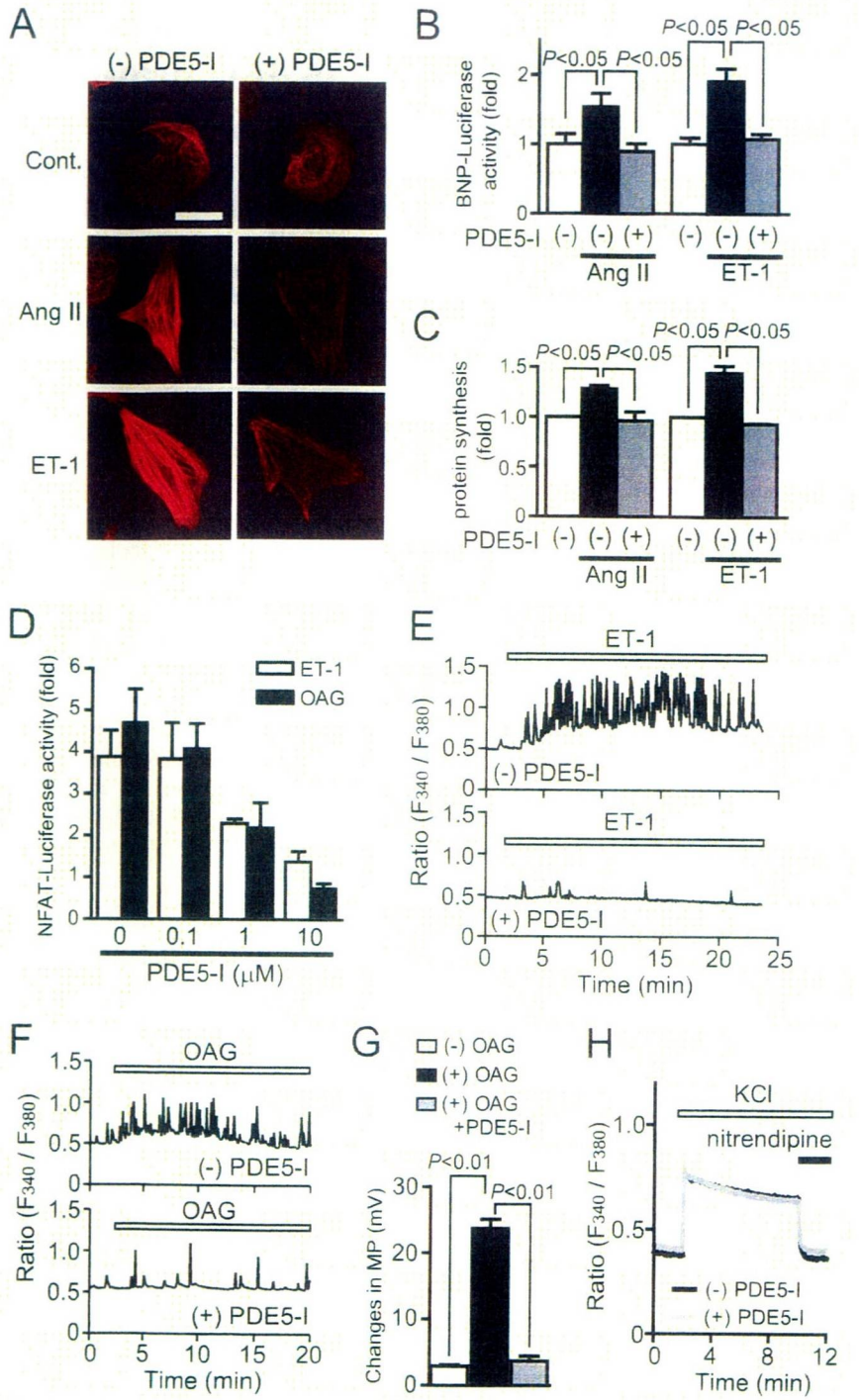

FIGURE 1. **Inhibition of PDE5 suppresses agonist-induced cardiomyocyte hypertrophic responses through inhibition of DAG-mediated Ca^{2+} signaling.** *A–C*, effects of PDE5-I on agonist-induced hypertrophic responses (actin reorganization (*A*), BNP expression (*B*), and protein synthesis (*C*)). Cardiomyocytes were treated with PDE5-I (10 μM) for 20 min before the addition of Ang II (1 μM) or ET-1 (100 nM). *Scale bar*, 50 μm. *D*, effects of PDE5-I on NFAT activation induced by ET-1 and OAG (30 μM). *E–H*, average time courses of Ca^{2+} responses induced by ET-1 (*E*), OAG (*F*), and KCl (*H*) in the absence or presence of PDE5-I. *G*, effects of PDE5-I on OAG-induced increase in membrane potential (*MP*). Cardiomyocytes were treated with OAG for 20 min, and maximal increase in MP was calculated from peak changes in $DiBAC_4(3)$ fluorescence intensity (21). *H*, voltage-dependent Ca^{2+} influx was evoked by KCl (8 mM) for 8 min, and nitrendipine (10 μM) was added to inhibit the activities of voltage-dependent Ca^{2+} channels.

only as a Ca^{2+}-permeable channel-forming subunit but also as an accessory protein to form the Ca^{2+} signaling complex (18). Endogenous TRPC1 and TRPC3 proteins are associated with each other to form native store-operated channels in HEK293 cells (19). In addition, diacylglycerol (DAG)-sensitive TRPC3, TRPC6, and TRPC7 proteins assemble to homotetramers or heterotetramers that function as DAG-activated cation channels (20). We have previously reported that TRPC3 and TRPC6 mediate Ang II-induced membrane depolarization, followed by Ca^{2+} influx through voltage-dependent Ca^{2+} channels in rat neonatal cardiomyocytes (21). Either knockdown of TRPC3 or TRPC6 channels completely suppressed Ang II-induced hypertrophy. Thus, TRPC1, TRPC3, and TRPC6 may form multimers in cardiomyocytes, which function as DAG-activated cation channels. Furthermore, we have recently demonstrated that treatment with a TRPC3 channel-selective blocker suppresses mechanical stretch-induced NFAT activation and pressure overload-induced cardiac hypertrophy in mice (22). Thus, inhibition of TRPC3-containing multimeric channels may represent a novel therapeutic strategy for preventing cardiac hypertrophy.

Phosphorylation of TRPC channels has been reported to modulate channel activity (23–25). For example, Fyn, an Src family Tyr kinase, physically interacts with the N-terminal region of TRPC6 proteins, and Tyr phosphorylation of TRPC6 enhances its channel activity (23). It has also been demonstrated that Src-dependent Tyr phosphorylation of TRPC3 is essential for DAG-activated cation influx (24). In contrast, Ser/Thr phosphorylation of TRPC3 channel attenuates its channel activity (25). Activation of PKG is known to regulate $[Ca^{2+}]_i$ at multiple levels (26). PKG activation by a NO donor or cGMP analog has been reported to inhibit voltage-dependent L-type Ca^{2+} channels by α_1-adrenergic receptor stimulation in cardiomyocytes (27). Several reports have shown that TRPC3 and TRPC6 channel activities are greatly attenuated by PKG-catalyzed phosphorylation of TRPC6 at threonine 69 (Thr^{69}) and TRPC3 at Thr^{11} and Ser^{263} (25, 28). The physiological importance of negative regulation of TRPC6 channels by the NO-

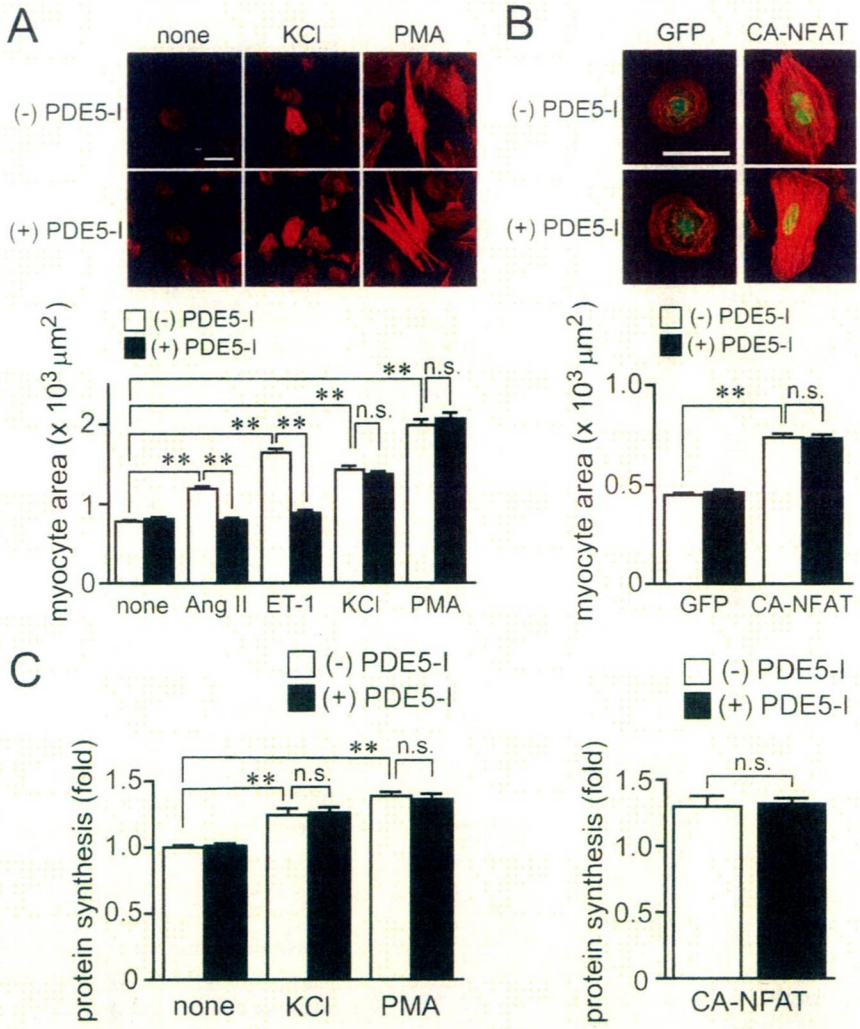

FIGURE 2. **Inhibition of PDE5 does not suppress the agonist-independent cardiomyocyte hypertrophic responses.** *A* and *C*, effects of PDE5-I on hypertrophic responses (actin reorganization, protein synthesis, and increases in area of cardiomyocytes) induced by KCl and phorbol 12-myristrate 13-acetate (*PMA*). Cardiomyocytes were stimulated with Ang II (1 μM), ET-1 (100 nM), KCl (5 mM), or phorbol 12-myristrate 13-acetate (1 μM) for 48 h. *B* and *C*, effects of PDE5-I on hypertrophic growth (*B*) and protein synthesis (*C*) in green fluorescent protein- and CA-NFAT-expressing cardiomyocytes. *Scale bar*, 50 μm. **, $p < 0.01$; *n.s.*, no significance.

cGMP-protein kinase G (PKG) signaling pathway has been reported in vascular smooth muscle cells (28). However, the role of PKG-dependent negative regulation of TRPC6 channels in the heart is still unknown.

Inhibition of cGMP-dependent phosphodiesterase 5 (PDE5) enhances basal PKG activity through an increase in intracellular cGMP concentration. In fact, chronic treatment with sildenafil, a PDE5 inhibitor, exhibits the anti-hypertrophic effects in mice (29, 30) and in patients with systolic heart failure (31). It has been reported that RGS2 mediates cardiac compensation to pressure overload and anti-hypertrophic effects of PDE5 inhibition in mice (32). Because PKG-dependent phosphorylation of RGS2 enhances GTPase activity of the α-subunit of G_q protein ($G\alpha_q$), this may explain the cGMP-dependent disruption of intracellular Ca^{2+} signaling induced by G_q-coupled receptor stimulation. However, we here found that inhibition of PDE5 also suppresses Ca^{2+} responses induced by the DAG analog and mechanical stretch (which may not require the activation of $G\alpha_q$ signaling) in rat neonatal cardiomyocytes. We also demonstrate that inhibition of PDE5 actually induces phosphorylation of TRPC6 proteins at Thr^{69}, leading to inhibition of TRPC6-mediated Ca^{2+} signaling. These results suggest that PKG-dependent inhibition of TRPC6 channel activity is required for the anti-hypertrophic effects of PDE5 inhibition.

EXPERIMENTAL PROCEDURES

Materials and Cell Cultures—A PDE5-selective inhibitor (PDE5-I; 4-{[3′,4′-(methylenedioxy)benzyl]amino}-6-methoxyquinazoline), 4-methyl-4′-[3,5-bis(trifluoromethyl)-1H-pyrazol-1-yl]-1,2,3-thiadiazole-5-carboxanilide (BTP2), and KT5823 were purchased from Calbiochem. 8-Bromo-cGMP (8-Br-cGMP), phorbol 12-myristrate 13-acetate, *S*-nitroso-*N*-acetyl-DL-penicillamine, 1-oleoyl-2-acetyl-*sn*-glycerol (OAG), and ET-1 were from Sigma. Ang II was from Peptide Lab. Fura2/AM was from Dojindo. Bis(1,3-dibutylbarbituric acid)trimethine oxonol ($DiBAC_4(3)$) was from Molecular Probes. Collagenase and Fugene 6 were from Roche Applied Science. Stealth small interfering RNA (siRNA) oligonucleotides, Alexa Fluor 568 phalloidin, and Lipofectamine 2000 were purchased from Invitrogen. Revatio (sildenafil citrate) was from Pfizer. The cDNAs coding a dominant negative mutant of TRPC6 (DN-TRPC6) and the TRPC6 (T69A) mutant were constructed as described (21, 28). Anti-TRPC6 was from Alomone. Phospho-Thr^{69} TRPC6 antiserum was generated against phospho-TRPC6 peptide (CHRRQ(P)TILREK). The phospho-TRPC6 antibody was purified by an antigen column. Isolation of rat neonatal cardiomyocytes and adenoviral infection of LacZ, green fluorescent protein, wild type (WT) TRPC6, or DN-TRPC6 were described (33). For knockdown of rat RGS proteins, cells were transfected with siRNAs (100 nM each) for RGS2 (AGAAAUAGCUCAAACGGGUCUUCCA) and RGS4 (UUUGAAAGCUGCCAGUCCACAUUCA) or control scrambled siRNAs for RGS2 (UUCACGGAACCGACCUUAAAUA) and RGS4 (AAAUAGCGUCUGACCACCCUUAGGU), using Lipofectamine 2000 for 72 h.

Reporter Activity—Measurement of NFAT-dependent luciferase activity and brain natriuretic peptide (BNP) promoter activity was performed as described previously (21). Briefly, cardiomyocytes (5×10^5 cells) plated on 24-well

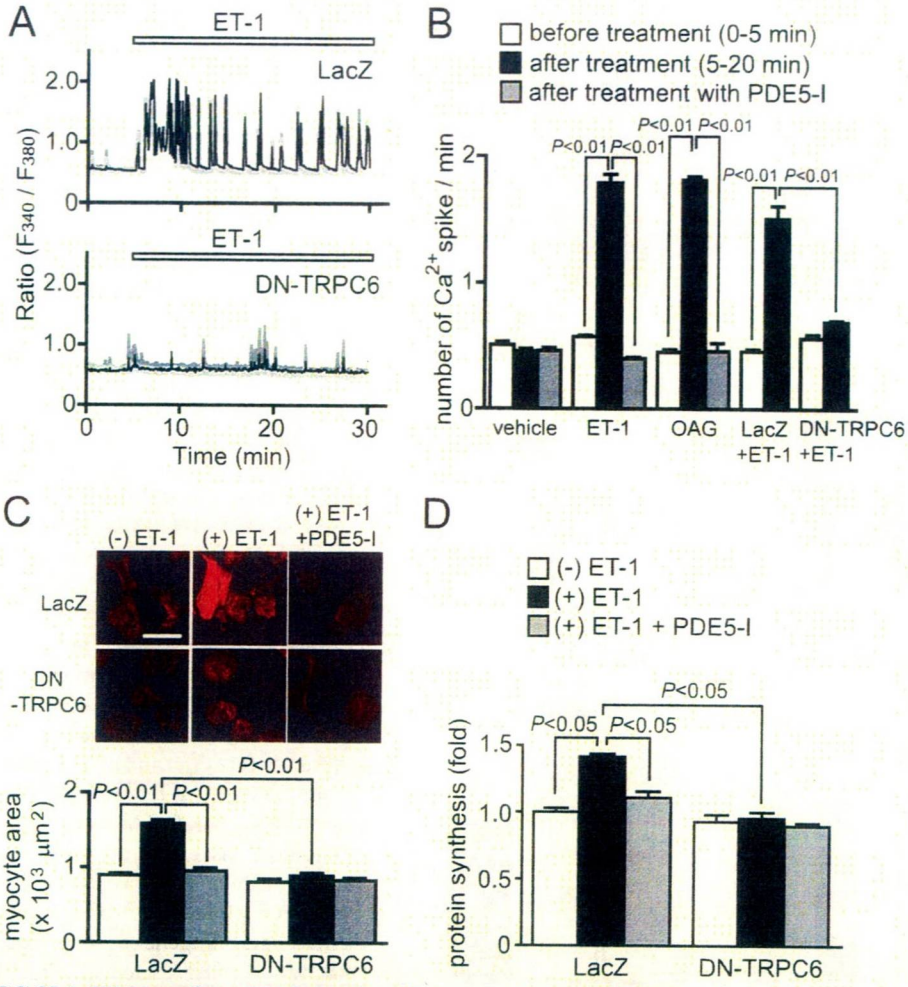

FIGURE 3. **TRPC6 mediates ET-1-induced cardiomyocyte hypertrophic responses.** *A*, Ca^{2+} responses induced by ET-1 (100 nM) in LacZ- and DN-TRPC6-overexpressing cardiomyocytes. *B*, results of the frequency of Ca^{2+} oscillations induced by ET-1 or OAG (30 μM). Cardiomyocytes were pretreated with PDE5-I (10 μM) 35 min before agonist stimulation. *C* and *D*, effects of DN-TRPC6 on ET-1-induced actin reorganization and increase in cell size (*C*) and protein synthesis (*D*). *Scale bar*, 50 μm.

dishes were transiently co-transfected with 0.45 μg of pNFAT-Luc and 0.05 μg of pRL-SV40 control plasmid or with 0.3 μg of pBNP-Luc and 0.2 μg of pRL-SV40 using Fugene 6. Expression of the constitutively active mutant of green fluorescent protein-fused NFAT proteins (CA-NFAT) was performed as described (34). Forty-eight h after transfection, cells were stimulated with Ang II (1 μM), ET-1 (100 nM), or mechanical stretch (21) for 6 h (for NFAT) or 24 h (for BNP).

Measurement of $[Ca^{2+}]_i$ and Membrane Potential—The intracellular Ca^{2+} concentration ($[Ca^{2+}]_i$) of cardiomyocytes or HEK293 cells was determined as described (35, 36). Briefly, HEK293 cells were transfected for 48 h with vector (pCI-neo), WT TRPC6, or TRPC6 (T69A) mutant using Fugene 6. Cardiomyocytes (1×10^6 cells) were plated on gelatin-coated glass bottom 35-mm dishes or on laminin-coated silicone rubber culture dishes (4 cm^2; STREX) and were loaded with 1 μM fura-2/AM at 37 °C for 30 min (37). As we measured the changes in $[Ca^{2+}]_i$ of the same cells before and after mechanical stretch, we treated cells with 20% of transient stretch for 3 s using automatic stretch systems (STB-150; STREX). Measurement and analysis of membrane potential were performed using $DiBAC_4(3)$ as described (21). The fluorescence intensity was measured with a video image analysis system (Aquacosmos, Hamamatsu Photonics).

Animal Models and Drug Treatment—All experiments on male C57BL6/J mice (C57BL6/J) were performed in accordance with the Guide for the Care and Use of Laboratory Animals prepared by Kyushu University. Sildenafil (100 mg/kg/day) was orally administered once a day for 1 week, and then hearts were removed and homogenized with radioimmune precipitation buffer.

Western Blot Analysis—TRPC6-expressing HEK293 cells (3×10^5 cells) or cardiomyocytes (1×10^6 cells) plated on 6-well dishes were directly harvested with 2× SDS sample buffer (200 μl). After centrifugation, supernatants (20–40 μl) were fractionated by 8% SDS-polyacrylamide gel and then transferred onto polyvinylidene difluoride membrane. For measurement of TRPC6 phosphorylation in mouse hearts, supernatants (100 μg of proteins) without boiling treatment were applied onto SDS-polyacrylamide gel. The expression and phosphorylation of endogenous TRPC6 proteins were detected by anti-TRPC6 (dilution rate, 1:1000) and anti-phospho-TRPC6 (1:1000) antibodies. We visualized the reactive bands using Supersignal® West Pico Luminol/Enhancer solution (Pierce). The optical density of the film was scanned and measured with Scion Image software.

Measurement of Hypertrophic Responses of Cardiomyocytes—Measurement of cardiomyocyte hypertrophy was performed as described (21, 34). Cardiomyocytes were fixed by paraformaldehyde and then stained with Alexa Fluor 548 phalloidin to visualize actin filaments. Digital photographs were taken at ×600 magnification with confocal microscopy (FV-10i, Olympus) or a Biozero microscope (BZ-8000, Keyence), and the average values of the cardiomyocyte area ($n > 100$ cells) were calculated using a BZ-II analyzer (Keyence). Protein synthesis was measured by [^{3}H]leucine incorporation. After cells were stimulated with Ang II or ET-1 for 2 h, [^{3}H]leucine (1 μCi/ml) was added to the culture medium and further incubated for 6 h. The incorporated [^{3}H]leucine was measured using a liquid scintillation counter.

Statistical Analysis—The results are shown as means ± S.E. All experiments were repeated at least three times. Statisti-

cal comparisons were made with a two-tailed Student's *t* test or analysis of variance followed by the Student-Newman-Keuls procedure with significance imparted at p values of <0.05.

RESULTS

Suppression of Diacylglycerol-mediated Ca^{2+} Responses by Inhibition of PDE5—We first investigated whether inhibition of PDE5 suppresses agonist-induced Ca^{2+} responses and hypertrophic responses in rat cardiomyocytes. Treatment with PDE5-I completely suppressed Ang II- or ET-1-induced hypertrophic responses, such as an increase in cell size, actin reorganization, hypertrophic gene (BNP) expression, and protein synthesis (Fig. 1, *A–C*). Stimulation of cardiomyocytes with ET-1 increases the frequency of Ca^{2+} oscillations through voltage-dependent Ca^{2+} channels (38). PDE5-I also suppressed ET-1-induced NFAT activation and oscillatory and sustained increase in $[Ca^{2+}]_i$ (Fig. 1, *D* and *E*). Although expression of CA-NFAT increased NFAT activity about 2.5-fold, this NFAT activation was not suppressed by PDE5-I (data not shown). These results suggest that PDE5-I inhibits NFAT activity through inhibition of Ca^{2+} responses. We have previously shown that DAG-sensitive TRPC channels (TRPC3 and TRPC6) mediate Ang II-induced activation of voltage-dependent Ca^{2+} influx through membrane depolarization (21). Treatment with OAG increased NFAT activity and the frequency of Ca^{2+} spikes, which were suppressed by PDE5-I (Fig. 1, *D* and *F*). In addition, the OAG-induced membrane depolarization, as determined by $DiBAC_4(3)$ imaging, was completely suppressed by PDE5-I pretreatment (Fig. 1*G*). Furthermore, nitrendipine-sensitive voltage-dependent Ca^{2+} influx-mediated increase in $[Ca^{2+}]_i$ induced by high KCl was not affected by PDE5-I pretreatment (Fig. 1*H*). In addition, the hypertrophic responses induced by high KCl (Fig. 2, *A* and *C*) or the expression of CA-NFAT (Fig. 2*B*) were not suppressed by PDE5 inhibition. Although DAG also activates protein kinase C-dependent hypertrophic signaling pathway (3), PDE5-I did not suppress the phorbol 12-myristrate 13-acetate-induced hypertrophic responses (Fig. 2, *A* and *C*). These results suggest that PDE5-I suppresses agonist-induced Ca^{2+} responses and cardiomyocyte hypertrophy through inhibition of DAG-mediated membrane depolarization.

Inhibition of TRPC6 Channel Activity by PDE5 Inhibition—To investigate the involvement of TRPC6 in agonist-induced cardiomyocyte hypertrophy, we used DN-TRPC6 (21). As shown in Fig. 3*A*, treatment of cardiomyocytes with ET-1 or OAG significantly increased the frequency of Ca^{2+} spikes, which were completely suppressed by PDE5 inhibition (Fig. 3, *A* and *B*). Expression of DN-TRPC6 also completely suppressed ET-1-induced increases in the frequency of Ca^{2+} spikes (Fig. 3, *A* and *B*) and hypertrophic responses (Fig. 3, *C* and *D*). The anti-hypertrophic effect of PDE5-I was completely abolished in DN-TRPC6-expressing myocytes, suggesting that PDE5-I suppresses the TRPC6-mediated hypertrophic signaling pathway.

Takahashi *et al.* (28) have recently reported that activation of the NO-cGMP-PKG pathway by extracellular treatment with a NO donor or cGMP analog inhibits TRPC6 channel activity through phosphorylation of $TRPC6$ at Thr^{69}. Thus,

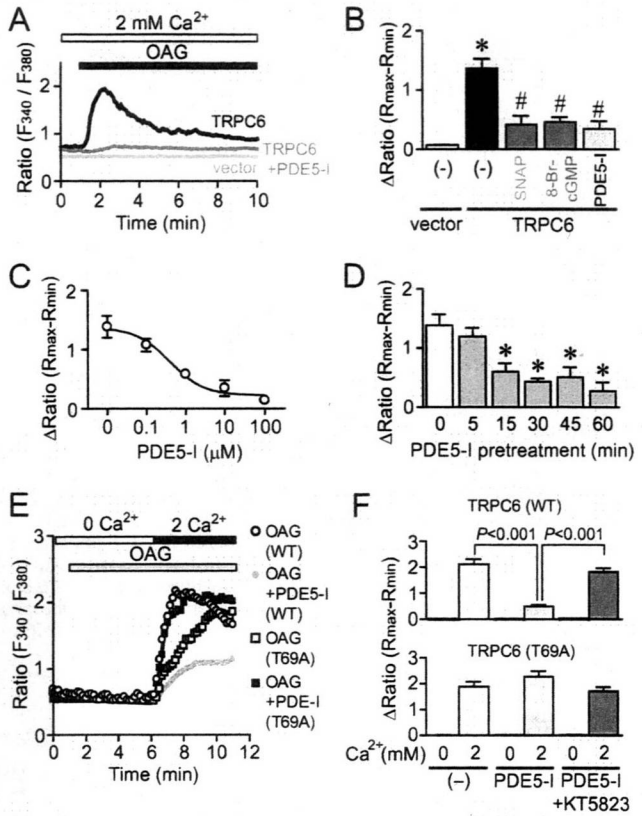

FIGURE 4. **PKG-dependent suppression of TRPC6-mediated Ca^{2+} influx by PDE5 inhibition.** *A*, average time courses of Ca^{2+} responses induced by OAG (30 μM) in vector and TRPC6-expressing HEK293 cells with or without PDE5-I. *B*, peak increases in $[Ca^{2+}]_i$ induced by OAG in vector- and TRPC6-expressing cells. HEK293 cells were treated with *S*-nitroso-*N*-acetyl-DL-penicillamine (*SNAP*) (100 μM), 8-Br-cGMP (100 μM), or PDE5-I (10 μM) for 30 min before the addition of OAG (30 μM). *C* and *D*, concentration-dependent (*C*) and time-dependent (*D*) suppression of OAG-induced $[Ca^{2+}]_i$ increases by PDE5-I. *E* and *F*, effects of PDE5-I on OAG-induced Ca^{2+} influx-mediated $[Ca^{2+}]_i$ increases in TRPC6 (WT)- and TRPC6 (T69A)-expressing cells. HEK293 cells were treated with KT5823 (1 μM) for 30 min before the addition of OAG. *, $p < 0.05$ *versus* vector (*white bar*); #, $p < 0.05$ *versus* TRPC6 (−) control (*black bar*).

we next examined whether PDE5 inhibition attenuates TRPC6 channel activity. Compared with vector-expressing HEK293 cells, treatment with OAG induced a marked increase in $[Ca^{2+}]_i$ of TRPC6-expressing cells (Fig. 4*A*). The TRPC6-mediated increase in $[Ca^{2+}]_i$ was significantly suppressed by pretreatment with PDE5-I as well as *S*-nitroso-*N*-acetyl-DL-penicillamine and 8-Br-cGMP (Fig. 4*B*). The IC_{50} value of inhibition of the TRPC6-mediated increase in $[Ca^{2+}]_i$ by PDE5-I was 0.41 ± 0.08 μM (Fig. 4*C*). More than 15 min of pretreatment with PDE5-I was required for the suppression of the TRPC6-mediated increase in $[Ca^{2+}]_i$ induced by OAG (Fig. 4*D*). PDE5-I suppressed the Ca^{2+} influx-mediated increase in $[Ca^{2+}]_i$ induced by OAG in TRPC6 (WT)-expressing cells, which was completely abolished by co-treatment with a PKG-selective inhibitor, KT5823 (Fig. 4, *E* and *F*). These results suggest that activation of PKG is required for the inhibition of TRPC6 channel activity. In fact, the suppression of OAG-induced Ca^{2+} influx by PDE5-I treatment was abolished in TRPC6 (T69A)-expressing cells. Thus, PKG-dependent phosphorylation of TRPC6 at Thr^{69} may be essential for inhibition of TRPC6 channel activity by PDE5 inhibition.

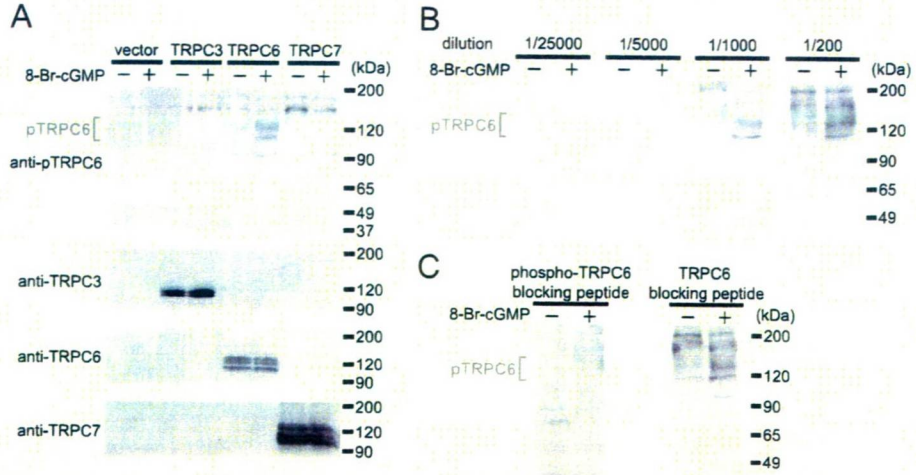

FIGURE 5. **Specific recognition of TRPC6 phosphorylation at Thr^{69} by a phospho-specific antibody.** *A*, phosphorylation of TRPC6 at Thr^{69} induced by PKG activation in vector-, TRPC3-, TRPC6-, and TRPC7-expressing HEK293 cells. HEK293 cells were treated with 8-Br-cGMP (100 μM) for 2 h. *B*, optimization of dilution of anti-phospho-TRPC6 antibody. Antibody (0.56 mg/ml) was diluted with Tris-buffered saline plus 0.1% Tween 20 (TBS-T) and incubated with blots for 1 h at room temperature. *C*, effect of treatment with a TRPC6-blocking peptide on the recognition of TRPC6 phosphorylation by this antibody. Blots were incubated with phospho-TRPC6 antibody diluted 1:1000 in TBS-T with phospho-TRPC6-blocking peptide or non-phosphorylated TRPC6-blocking peptide (10 μg/ml) for 1 h at room temperature.

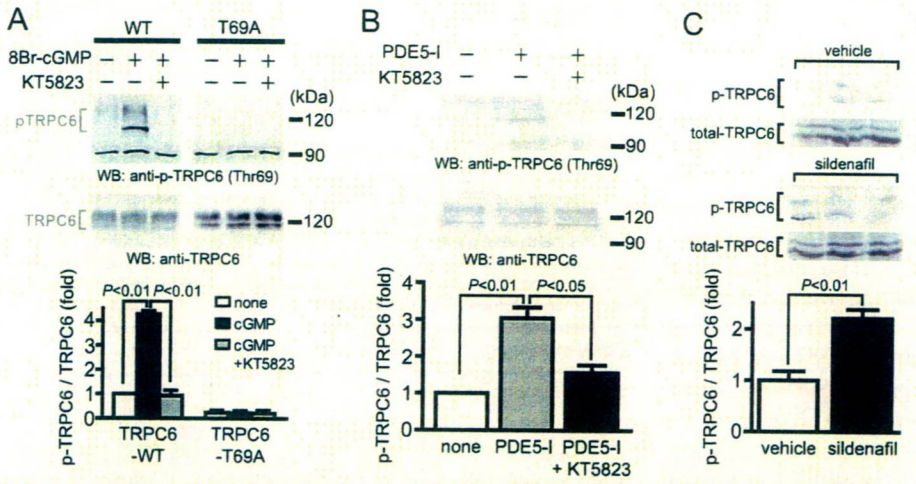

FIGURE 6. **PKG-dependent phosphorylation of Thr^{69} in TRPC6 by PDE5 inhibition.** *A*, PKG-dependent phosphorylation of TRPC6 proteins at Thr^{69} in TRPC6 (WT)- and TRPC6 (T69A)-expressing HEK293 cells. HEK293 cells were treated with KT5823 (1 μM) for 20 min before the addition of 8-Br-cGMP (100 μM) and PDE5-I (10 μM) for 30 min. *B*, PKG-dependent TRPC6 phosphorylation by PDE5-I. Cardiomyocytes were treated with KT5823 for 20 min before the addition of PDE5-I (10 μM) for 1 h. *C*, effects of sildenafil on the phosphorylation of TRPC6 in mice. One week after oral administration with sildenafil (100 mg/kg/day), hearts were lysed with radioimmune precipitation buffer, and 100 μg of proteins were applied to SDS-PAGE.

Phosphorylation of TRPC6 Proteins at Thr^{69} by PDE5 Inhibition—In order to examine whether inhibition of PDE5 actually induces phosphorylation of TRPC6 proteins in cardiomyocytes, we generated a phospho-specific TRPC6 (Thr^{69}) antibody. Because TRPC6 proteins have two glycosylation sites (39), a single 100 kDa band and smear 110–120 kDa bands due to several patterns of glycosylation were observed in TRPC6 wild type (WT)-overexpressing HEK293 cells (Fig. 5*A*). Phosphorylation of TRPC6 proteins was observed only when HEK293 cells were stimulated with 8-Br-cGMP. In contrast, this phosphorylation was not observed in vector-, TRPC3-, or TRPC7-expressing HEK293 cells, even when cells were stimulated with 8-Br-cGMP. The TRPC6 phosphorylation could be detectable when the antibody was diluted from 1,000- to 5,000-fold (Fig. 5*B*). Furthermore, the TRPC6 phosphorylation bands were completely abolished by the treatment with phospho-TRPC6-blocking peptide but not by control blocking peptide (Fig. 5*C*). These results clearly suggest that our phospho-specific TRPC6 antibody specifically recognized the phosphorylation of rodent TRPC6 at Thr^{69}.

Activation of PKG by 8-Br-cGMP and PDE5-I stimulated the phosphorylation of TRPC6 proteins, which was completely suppressed by the treatment with KT5823 in TRPC6-WT-expressing HEK293 cells (Fig. 6, *A* and *B*). The PKG-mediated TRPC6 phosphorylation was not observed in TRPC6 (T69A)-expressing cells, indicating the specificity of this antibody. Treatment with PDE5-I significantly increased the phosphorylation of native TRPC6 proteins in rat cardiomyocytes, which was completely suppressed by KT5823 (Fig. 6*B*). We further examined whether inhibition of PDE5 actually phosphorylates TRPC6 proteins *in vivo*. Takimoto *et al.* (29) have previously reported that chronic treatment with sildenafil (100 mg/kg/day) prevents and reverses cardiac hypertrophy induced by pressure overload in mice. We found that oral treatment with sildenafil (100 mg/kg/day) for 1 week, under the same conditions as in their report, actually increases TRPC6 phosphorylation levels in mouse hearts (Fig. 6*C*).

Inhibition of TRPC6 Phosphorylation at Thr^{69} Diminishes the Anti-hypertrophic Effects of PDE5 Inhibition—Overexpression of TRPC6 (T69A) enhanced the increase in NFAT activity and BNP expression induced by ET-1, which was not suppressed by PDE5-I (Fig. 7, *A* and *B*). In addition, expression of TRPC6 (WT) or TRPC6 (T69A) enhanced the ET-1-induced hypertrophic responses of cardiomyocytes (Fig. 7, *C* and *D*). Although PDE5-I completely suppressed the ET-1-induced hypertrophic responses in control (vector)- or TRPC6 (WT)-expressing cardiomyocytes, PDE5-I did not suppress hypertrophic responses in TRPC6 (T69A)-expressing cardiomyocytes. These results suggest that inhibition of TRPC6 channel activity via its PKG-dependent phosphorylation at Thr^{69} participates in anti-cardiomyocyte hypertrophic effects of PDE5 inhibition.

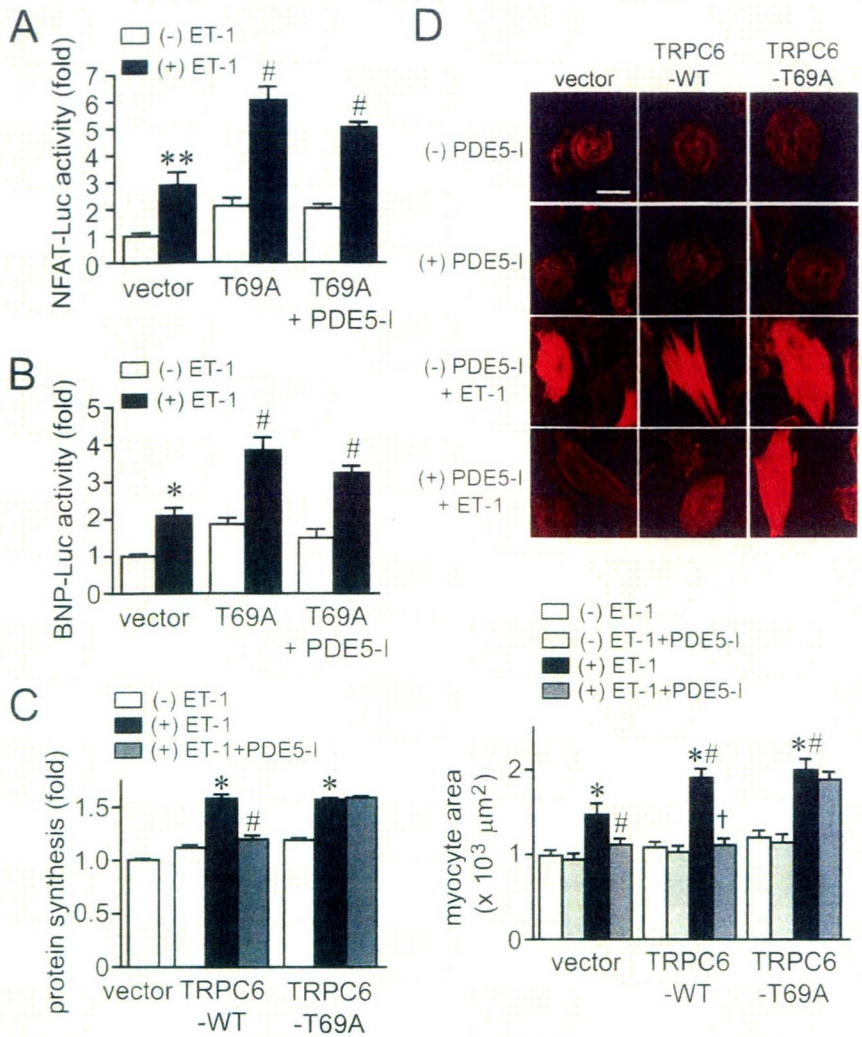

FIGURE 7. **Phosphorylation of Thr^{69} is essential for the anti-hypertrophic effects of PDE5 inhibition.** *A* and *B*, effects of PDE5-I on ET-1-induced NFAT activation (*A*) and BNP gene expression (*B*) in TRPC6 (T69A)-expressing cardiomyocytes. *C* and *D*, effects of PDE5-I on the ET-1-induced protein synthesis (*C*) and increase in the size of TRPC6 (T69A)-overexpressing cardiomyocytes (*D*). Cardiomyocytes were treated with PDE5-I (10 μM) for 20 min before the addition of ET-1 (100 nM). *Scale bar*, 50 μm. *, $p < 0.05$; **, $p < 0.01$ *versus* without (−) ET-1 within vector. #, $p < 0.05$ *versus* vector with (+) ET-1. †, $p < 0.01$ *versus* TRPC6-WT with ET-1.

Suppression of Mechanical Stretch-induced Ca^{2+} Responses by PDE5 Inhibition—Because mechanical stress is also involved in the development of cardiac hypertrophy, we next examined whether PDE5-I inhibits Ca^{2+} responses induced by mechanical stretch. In control cardiomyocytes, a periodic increase in $[Ca^{2+}]_i$ was observed after cells were stretched by 20% for 3 s with a speed of 20 mm/s (Fig. 8*A*). A bis(triluoromethyl)pyrazole derivative, BTP2, is recently used as a selective inhibitor of the TRPC1 to -7 channels. We previously reported that BTP2 at 3 μM suppresses TRPC6-mediated Ca^{2+} influx by 80% in HEK293 cells (22). Treatment with PDE5-I or BTP2 abolished mechanical stretch-induced increase in $[Ca^{2+}]_i$ (Fig. 8*A*). Mechanical stretch-induced increases in NFAT-dependent luciferase activity, BNP-luciferase activity, and protein synthesis were suppressed by PDE5-I, which was canceled by co-treatment with KT5823 (Fig. 8, *B–D*). We also found that mechanical stretch-induced increases in $[Ca^{2+}]_i$, NFAT activation, and hypertrophic responses were completely suppressed by the expression of DN-TRPC6 (Fig. 8, *B–D*). These results suggest that PDE5-I suppresses mechanical stretch-induced Ca^{2+} responses linked to cardiomyocyte hypertrophic responses through inhibition of TRPC6 channels.

Knockdown of RGS2 and RGS4 Does Not Affect the Effect of PDE5-I—It has been recently reported that PKG-dependent phosphorylation of RGS2 and RGS4 mediates the anti-hypertrophic effects in mouse hearts (32, 40, 41). Thus, we next examined the involvement of RGS proteins in the inhibition of agonist-induced Ca^{2+} responses by PDE5 inhibition, using siRNAs for RGS2 and RGS4. We confirmed that the treatment of cardiomyocytes with siRNAs for RGS2/4 reduced the expression levels of RGS2 and RGS4 mRNAs to 18.5 ± 5.2 and 26.7 ± 7.8%, respectively. Knockdown of RGS2/4 proteins did not affect Ca^{2+} responses and NFAT activation induced by ET-1 (Fig. 9). The addition of extracellular Ca^{2+} induced a Ca^{2+} influx-mediated increase in $[Ca^{2+}]_i$ by ET-1 stimulation, which was significantly suppressed by PDE5-I treatment in control myocytes (Fig. 9, *A–C*). The Ca^{2+} influx-mediated $[Ca^{2+}]_i$ increases and increase in NFAT activity by agonist stimulation were slightly enhanced in RGS2/4-deficient myocytes and were also significantly suppressed by PDE5-I treatment (Fig. 9, *B–D*). These results suggest that RGS2 and RGS4 proteins are not mainly involved in the inhibition of agonist-induced Ca^{2+} responses by PDE5 inhibition in cardiomyocytes.

DISCUSSION

In this study, we have demonstrated that inhibition of PDE5 suppresses agonist-induced and mechanical stretch-induced hypertrophic responses in rat cardiomyocytes. The increases in the frequency of Ca^{2+} oscillations induced by OAG or mechanical stretch are greatly attenuated by PDE5 inhibition. PDE5-I suppresses OAG-induced membrane depolarization, suggesting the inhibition of DAG-sensitive TRPC channels by PDE5 inhibitor. Treatment with PDE5-I actually induces PKG-dependent phosphorylation of TRPC6 proteins at Thr^{69} and inhibits TRPC6-mediated Ca^{2+} responses. Because the inhibition of ET-1-induced hypertrophic responses by PDE5-I was abolished in TRPC6 (T69A)-expressing cardiomyocytes, we suggest that phosphorylation of TRPC6 is required for

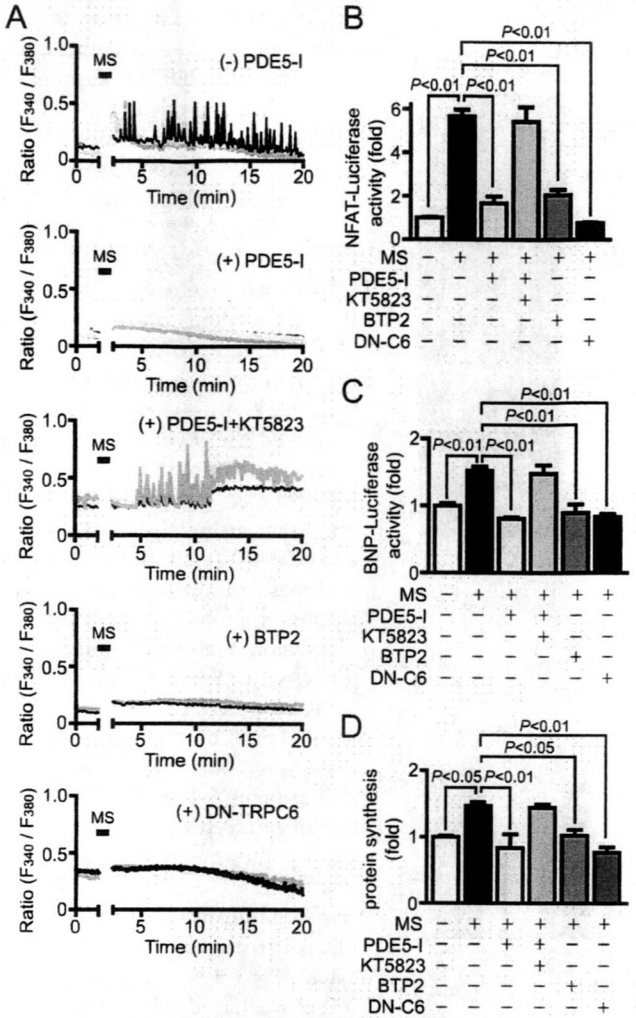

FIGURE 8. **Inhibition of PDE5 suppresses Ca^{2+} responses and cardiomyocyte hypertrophic responses induced by mechanical stretch.** *A*, typical traces of Ca^{2+} responses induced by mechanical stretch (*MS*) in the absence or presence of PDE5-I, KT5823, or BTP2. Cardiomyocytes were treated with PDE5-I (10 μM) or BTP2 (5 μM) for 35 min before MS. DN-TRPC6 proteins were expressed using adenoviral infection. *B–D*, effects of PDE5-I, BTP2, and DN-TRPC6 on the MS-induced NFAT activation (*B*) and hypertrophic responses (BNP gene expression (*C*) and protein synthesis (*D*)).

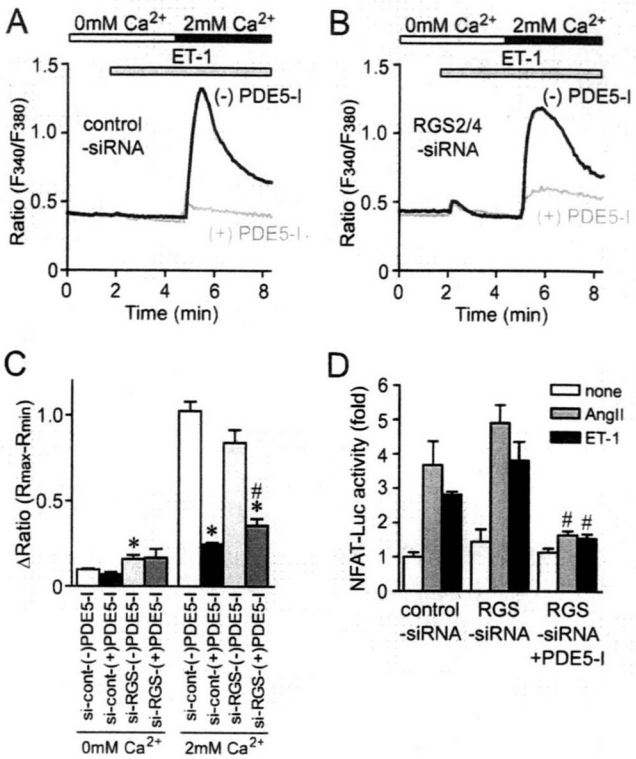

FIGURE 9. **PDE5-I suppresses ET-1-induced Ca^{2+} responses in RGS2/4-down-regulated cardiomyocytes.** *A* and *B*, average time courses of Ca^{2+} responses induced by ET-1 in the absence or presence of PDE5-I in control siRNA-treated cardiomyocytes (*A*) and RGS2/4 siRNAs-treated cardiomyocytes (*B*). *C*, peak Ca^{2+} releases (0 mM Ca^{2+}) and Ca^{2+} influx-mediated increases in $[Ca^{2+}]_i$ (2 mM Ca^{2+}) induced by ET-1 (100 nM). *D*, effects of knockdown of RGS2/4 proteins on PKG-dependent inhibition of ET-1-induced NFAT activation by PDE5-I. *, $p < 0.05$ *versus* control siRNA-treated cardiomyocytes without PDE5-I; #, $p < 0.05$ *versus* RGS2/4 siRNA-treated cardiomyocytes without PDE5-I.

the anti-hypertrophic effects of PDE5 inhibition. In addition, PDE5-I-induced suppression of Ca^{2+} influx induced by ET-1 was not abolished by the knockdown of RGS2 and RGS4, both of which are reported to be activated by PKG. This result emphasizes the physiological importance of TRPC6 phosphorylation by PDE5-I in suppressing Ca^{2+} influx induced by agonist stimulation and mechanical stretch.

Higazi *et al.* (38) has recently reported that inositol-1,4,5-trisphosphate-induced Ca^{2+} release from perinuclear inositol-1,4,5-trisphosphate receptors by ET-1 stimulation or membrane depolarization preferentially couples to the calcineurin/NFAT pathway to induce hypertrophy. They have also demonstrated that the potentiation of Ca^{2+} influx activity induced by isoproterenol or BayK8644 induces activation of calcineurin/NFAT signaling pathway via Ca^{2+} release from perinuclear inositol-1,4,5-trisphosphate receptors. This mechanism may be involved in the process of voltage-dependent Ca^{2+} influx-mediated NFAT activation evoked by TRPC6 activation. Although we did not measure nuclear Ca^{2+} concentrations, PDE5-I may inhibit the increase in nuclear Ca^{2+} concentrations because PDE5-I suppresses NFAT activation induced by ET-1.

Because PDE5-I did not suppress the high KCl-induced increase in $[Ca^{2+}]_i$ (Fig. 1), we suggest that PKG activation by PDE5-I does not inhibit L-type Ca^{2+} channels. In contrast, Fiedler *et al.* (27) have reported that overexpression of PKG type I suppresses single L-type Ca^{2+} channel open probability and $[Ca^{2+}]_i$ transient amplitude. This discrepancy can be explained by the intensity of PKG activation. Although we show that PDE5-I increased the TRPC6 phosphorylation level about 3-fold, the treatment with 8-Br-cGMP induced a more than 5-fold increase in TRPC6 phosphorylation level (data not shown). This suggests that PDE5-I moderately activates PKG, and this activation is insufficient to inhibit L-type Ca^{2+} channel activity.

Inhibition of PDE5 suppresses mechanical stretch-induced Ca^{2+} responses in cardiomyocytes. Because the pattern of Ca^{2+} spikes is similar to those induced by ET-1 or OAG stimulation, membrane depolarization may be also involved in this mechanism. This idea is supported by the reports that DAG-sensitive TRPC channels work as stretch-

activated depolarizing channels in the vascular system (42–44). It has recently been reported that TRPC6 is activated by mechanical stretch through two pathways: G protein-mediated indirect activation and direct activation of TRPC6 (42). Furthermore, TRPC6 can be synergistically activated by mechanical force in the presence of G_q-coupled receptor stimulation (43). We have previously reported that mechanical stretch increases the concentration of extracellular nucleotides, which stimulate G_q protein-coupled P2Y receptors (37). Thus, extracellular nucleotides released by mechanical stretch and mechanical force may synergistically increase TRPC6 channel activity in rat neonatal cardiomyocytes.

Because Kwan *et al.* (25) reported that the activation of PKG by NO donor and 8-Br-cGMP increases phosphorylation at Thr^{11} and Ser^{263} of human TRPC3 proteins, it is possible that inhibition of PDE5 also results in phosphorylation of TRPC3 proteins and reduction of TRPC3 channel activity. Although Ser^{263} of human TRPC3 protein is conserved among humans, rats, and mice, Thr^{11} is not present in mouse and rat TRPC3 proteins. We have tried to generate an antibody to recognize the phosphorylated form of Ser^{263} in TRPC3 but failed to obtain the useful antibody. However, we confirmed that PDE5-I inhibits TRPC3-mediated Ca^{2+} influx induced by OAG in TRPC3-expressing HEK293 cells, which was abolished in TRPC3 (S325A)-expressing HEK293 cells (n = 2; data not shown). Because the Ser^{325} in mouse TRPC3 protein is identical to Ser^{263} in human TRPC3 protein, this result implies that the inhibition of TRPC3 channel activity by PDE-I may also be involved in the anti-hypertrophic effects of PDE5 inhibition.

We have not yet been able to identify the individual roles of TRPC6 and TRPC3 channels in cardiomyocytes. Despite their high degree of structural and functional similarity, TRPC3, TRPC6, and TRPC7 are substantially different in their basal channel activities (45). The basal channel activity of TRPC6 is tightly regulated (39). In contrast, TRPC3 and TRPC7 have considerable constitutive activity when expressed in various cell lines (46). Despite the low basal activity of TRPC6 channels, results from transgenic mice with cardiomyocyte-specific expression of TRPC3 or TRPC6 channels show that the up-regulation of TRPC6 channel proteins is essential for the development of cardiac hypertrophy (13, 14). In pathological conditions, hearts are exposed to mechanical stress and neurohumoral factors. Therefore, a characteristic of TRPC6 channels that is synergistically activated by mechanical stretch in the presence of a low concentration of agonist (43) may explain the mechanism of induction of pathological hypertrophy. Because TRPC3 has high constitutive activity among the DAG-activated TRPC3/6/7 family and is up-regulated in smooth muscle cells from TRPC6-deficient mice (45), the TRPC6-deficient mouse heart may cause excessive hypertrophy by pressure overload like a TRPC3-transgenic mouse heart (13). In addition, there is no pharmacological tool that selectively inhibits TRPC6 channel activity. Generation of transgenic mice with heart-specific expression of the dominant negative TRPC6 mutant, which moderately inhibits the function of TRPC6 channels without any compensation, will be necessary for understanding the pathophysiological role of TRPC6 in the heart.

In conclusion, we demonstrated that inhibition of DAG-sensitive TRPC channel activities through PKG-dependent phosphorylation is required for the anti-hypertrophic effects of PDE5 inhibition in rat cardiomyocytes. Our finding will provide a new insight for the creation of therapeutic strategies for heart failure.

Acknowledgments—We thank Marina Ariyoshi and Shinji Oda for measurement of Ca^{2+} imaging during the early stage of this study. We also thank Dr. Koichiro Kuwahara (Kyoto University) for helpful comments.

REFERENCES

1. Mann, D. L. (1999) *Circulation* **100,** 999–1008
2. Dorn, G. W., 2nd, and Force, T. (2005) *J. Clin. Invest.* **115,** 527–537
3. Heineke, J., and Molkentin, J. D. (2006) *Nat. Rev. Mol. Cell Biol.* **7,** 589–600
4. Liao, X. D., Tang, A. H., Chen, Q., Jin, H. J., Wu, C. H., Chen, L. Y., and Wang, S. Q. (2003) *Biochem. Biophys. Res. Commun.* **310,** 405–411
5. Molkentin, J. D., Lu, J. R., Antos, C. L., Markham, B., Richardson, J., Robbins, J., Grant, S. R., and Olson, E. N. (1998) *Cell* **93,** 215–228
6. Frey, N., McKinsey, T. A., and Olson, E. N. (2000) *Nat. Med.* **6,** 1221–1227
7. Ramirez, M. T., Zhao, X. L., Schulman, H., and Brown, J. H. (1997) *J. Biol. Chem.* **272,** 31203–31208
8. Song, K., Backs, J., McAnally, J., Qi, X., Gerard, R. D., Richardson, J. A., Hill, J. A., Bassel-Duby, R., and Olson, E. N. (2006) *Cell* **125,** 453–466
9. Berridge, M. J., Bootman, M. D., and Roderick, H. L. (2003) *Nat. Rev. Mol. Cell Biol.* **4,** 517–529
10. Colella, M., Grisan, F., Robert, V., Turner, J. D., Thomas, A. P., and Pozzan, T. (2008) *Proc. Natl. Acad. Sci. U.S.A.* **105,** 2859–2864
11. Large, W. A. (2002) *J. Cardiovasc. Electrophysiol.* **13,** 493–501
12. Yao, X., and Garland, C. J. (2005) *Circ. Res.* **97,** 853–863
13. Nakayama, H., Wilkin, B. J., Bodi, I., and Molkentin, J. D. (2006) *FASEB J.* **20,** 1660–1670
14. Kuwahara, K., Wang, Y., McAnally, J., Richardson, J. A., Bassel-Duby, R., Hill, J. A., and Olson, E. N. (2006) *J. Clin. Invest.* **116,** 3114–3126
15. Nishida, M., and Kurose, H. (2008) *Naunyn Schmiedebergs Arch. Pharmacology* **378,** 395–406
16. Bush, E. W., Hood, D. B., Papst, P. J., Chapo, J. A., Minobe, W., Bristow, M. R., Olson, E. N., and McKinsey, T. A. (2006) *J. Biol. Chem.* **281,** 33487–33496
17. Seth, M., Zhang, Z. S., Mao, L., Graham, V., Burch, J., Stiber, J., Tsiokas, L., Winn, M., Abramowitz, J., Rockman, H. A., Birnbaumer, L., and Rosenberg, P. (2009) *Circ. Res.* **105,** 1023–1030
18. Mori, Y., Wakamori, M., Miyakawa, T., Hermosura, M., Hara, Y., Nishida, M., Hirose, K., Mizushima, A., Kurosaki, M., Mori, E., Gotoh, K., Okada, T., Fleig, A., Penner, R., Iino, M., and Kurosaki, T. (2002) *J. Exp. Med.* **195,** 673–681
19. Zagranichnaya, T. K., Wu, X., and Villereal, M. L. (2005) *J. Biol. Chem.* **280,** 29559–29569
20. Hofmann, T., Schaefer, M., Schultz, G., and Gudermann, T. (2002) *Proc. Natl. Acad. Sci. U.S.A.* **99,** 7461–7466
21. Onohara, N., Nishida, M., Inoue, R., Kobayashi, H., Sumimoto, H., Sato, Y., Mori, Y., Nagao, T., and Kurose, H. (2006) *EMBO J.* **25,** 5305–5316
22. Kiyonaka, S., Kato, K., Nishida, M., Mio, K., Numaga, T., Sawaguchi, Y., Yoshida, T., Wakamori, M., Mori, E., Numata, T., Ishii, M., Takemoto, H., Ojida, A., Watanabe, K., Uemura, A., Kurose, H., Morii, T., Kobayashi, T., Sato, Y., Sato, C., Hamachi, I., and Mori, Y. (2009) *Proc. Natl. Acad. Sci. U.S.A.* **106,** 5400–5405
23. Hisatsune, C., Kuroda, Y., Nakamura, K., Inoue, T., Nakamura, T., Michikawa, T., Mizutani, A., and Mikoshiba, K. (2004) *J. Biol. Chem.* **279,** 18887–18894
24. Vazquez, G., Wedel, B. J., Kawasaki, B. T., Bird, G. S., and Putney, J. W., Jr.

(2004) *J. Biol. Chem.* **279,** 40521–40528
25. Kwan, H. Y., Huang, Y., and Yao, X. (2004) *Proc. Natl. Acad. Sci. U.S.A.* **101,** 2625–2630
26. Kass, D. A., Champion, H. C., and Beavo, J. A. (2007) *Circ. Res.* **101,** 1084–1095
27. Fiedler, B., Lohmann, S. M., Smolenski, A., Linnemuller, S., Pieske, B., Schroder, F., Molkentin, J. D., Drexler, H., and Wollert, K. C. (2002) *Proc. Natl. Acad. Sci. U.S.A.* **99,** 11363–11368
28. Takahashi, S., Lin, H., Geshi, N., Mori, Y., Kawarabayashi, Y., Takami, N., Mori, M. X., Honda, A., and Inoue, R. (2008) *J. Physiol.* **586,** 4209–4223
29. Takimoto, E., Champion, H. C., Li, M., Belardi, D., Ren, S., Rodriguez, E. R., Bedja, D., Gabrielson, K. L., Wang, Y., and Kass, D. A. (2005) *Nat. Med.* **11,** 214–222
30. Hsu, S., Nagayama, T., Koitabashi, N., Zhang, M., Zhou, L., Bedja, D., Gabrielson, K. L., Molkentin, J. D., Kass, D. A., and Takimoto, E. (2009) *Cardiovasc. Res.* **81,** 301–309
31. Lewis, G. D., Lachmann, J., Camuso, J., Lepore, J. J., Shin, J., Martinovic, M. E., Systrom, D. M., Bloch, K. D., and Semigran, M. J. (2007) *Circulation* **115,** 59–66
32. Takimoto, E., Koitabashi, N., Hsu, S., Ketner, E. A., Zhang, M., Nagayama, T., Bedja, D., Gabrielson, K. L., Blanton, R., Siderovski, D. P., Mendelsohn, M. E., and Kass, D. A. (2009) *J. Clin. Invest.* **119,** 408–420
33. Nishida, M., Maruyama, Y., Tanaka, R., Kontani, K., Nagao, T., and Kurose, H. (2000) *Nature* **408,** 492–495
34. Nishida, M., Onohara, N., Sato, Y., Suda, R., Ogushi, M., Tanabe, S., Inoue, R., Mori, Y., and Kurose, H. (2007) *J. Biol. Chem.* **282,** 23117–23128
35. Nishida, M., Sugimoto, K., Hara, Y., Mori, E., Morii, T., Kurosaki, T., and Mori, Y. (2003) *EMBO J.* **22,** 4677–4688
36. Nishida, M., Tanabe, S., Maruyama, Y., Mangmool, S., Urayama, K., Nagamatsu, Y., Takagahara, S., Turner, J. H., Kozasa, T., Kobayashi, H., Sato, Y., Kawanishi, T., Inoue, R., Nagao, T., and Kurose, H. (2005) *J. Biol. Chem.* **280,** 18434–18441
37. Nishida, M., Sato, Y., Uemura, A., Narita, Y., Tozaki-Saitoh, H., Nakaya, M., Ide, T., Suzuki, K., Inoue, K., Nagao, T., and Kurose, H. (2008) *EMBO J.* **27,** 3104–3115
38. Higazi, D. R., Fearnley, C. J., Drawnel, F. M., Talasila, A., Corps, E. M., Ritter, O., McDonald, F., Mikoshiba, K., Bootman, M. D., and Roderick, H. L. (2009) *Mol. Cell* **33,** 472–482
39. Dietrich, A., Mederos y Schnitzler, M., Emmel, J., Kalwa, H., Hofmann, T., and Gudermann, T. (2003) *J. Biol. Chem.* **278,** 47842–47852
40. Huang, J., Zhou, H., Mahavadi, S., Sriwai, W., and Murthy, K. S. (2007) *Am. J. Physiol. Cell Physiol.* **292,** C200–C208
41. Tokudome, T., Kishimoto, I., Horio, T., Arai, Y., Schwenke, D. O., Hino, J., Okano, I., Kawano, Y., Kohno, M., Miyazato, M., Nakao, K., and Kangawa, K. (2008) *Circulation* **117,** 2329–2339
42. Mederos y Schnitzler, M., Storch, U., Meibers, S., Nurwakagari, P., Breit, A., Essin, K., Gollasch, M., and Gudermann, T. (2008) *EMBO J.* **27,** 3092–3103
43. Inoue, R., Jensen, L. J., Jian, Z., Shi, J., Hai, L., Lurie, A. I., Henriksen, F. H., Salomonsson, M., Morita, H., Kawarabayashi, Y., Mori, M., Mori, Y., and Ito, Y. (2009) *Circ. Res.* **104,** 1399–1409
44. Gottlieb, P., Folgering, J., Maroto, R., Raso, A., Wood, T. G., Kurosky, A., Bowman, C., Bichet, D., Patel, A., Sachs, F., Martinac, B., Hamill, O. P., Honoré, E. (2008) *Pflugers Arch.* **455,** 1097–1103
45. Dietrich, A., Mederos Y Schnitzler, M., Gollasch, M., Gross, V., Storch, U., Dubrovska, G., Obst, M., Yildirim, E., Salanova, B., Kalwa, H., Essin, K., Pinkenburg, O., Luft, F. C., Gudermann, T., and Birnbaumer, L. (2005) *Mol. Cell. Biol.* **25,** 6980–6989
46. Trebak, M., Vazquez, G., Bird, G. S., and Putney, J. W., Jr. (2003) *Cell Calcium* **33,** 451–461

EXPERIMENTAL MEDICINE
実験医学 増刊

別　刷

羊土社

〒101-0052
東京都千代田区神田小川町2-5-1
TEL 03(5282)1211　FAX 03(5282)1212
E-mail：eigyo@yodosha.co.jp
URL：http://www.yodosha.co.jp/

2. ヒト幹細胞からの肝細胞分化誘導とその創薬非臨床試験への応用

佐藤陽治，石田誠一，鈴木和博，簾内桃子

今日の医薬品開発では，ヒトでの肝毒性および薬物体内動態・薬物相互作用を予測するための非臨床試験において，ヒト肝細胞・肝組織を用いた毒性試験および薬物動態・薬理試験を行うことが非常に重要だと認識されている．しかし，ヒト肝細胞・肝組織の入手の難しさ，個体差およびロット差の問題など，大きな問題点が依然として存在する．本稿では，これらの問題点について解説するとともに，その克服を目指し，ヒト多能性幹細胞から肝細胞を効率的に誘導して肝毒性・代謝研究に応用する試みについて述べる．

はじめに

生体の薬物に対する反応において，ヒトと動物との間にはきわめて大きな種差がある．その主な原因として，標的組織における反応性の相違と薬物の体内動態の相違があげられる．特に，薬物動態関連因子は実験動物とヒトとの間には著しく大きな種差があることが知られている．これらの種差のため，開発中の医薬品候補化合物がヒトでの臨床段階において思わぬ毒性を示したり，期待される薬物動態を示さなかったりするなどして，開発中止になることがある．そこで最近ではヒト細胞・組織を用いた非臨床試験が広く行われるようになった．医薬品開発の初期においてヒト細胞・組織を用いた非臨床試験を行うことは，開発にかかわる意思決定を早めることを可能とし，医薬品開発の効率化と経済性に資するとともに，結果として無駄な動物実験を省くことにも役立つ．

肝臓はヒト体内では最大の腺組織であり，代謝において中心的な役割を担い，健康な生命の維持に大きく寄与している．このため，薬物誘発性の肝機能障害（薬物性肝障害）は薬物に由来する副作用のなかでも医薬品開発の過程における開発中止，警告表示あるいは販売中止に至る主要な薬物関連有害事象の1つとなっている．したがって，医薬品開発においては，薬物およびその代謝産物のヒト肝臓に対する毒性を可能な限り早期に予測することが大切となる．また，薬物のヒト

[キーワード＆略語]
薬物性肝障害，特異体質，薬物代謝，個人差，幹細胞

ES細胞：embryonic stem cell（胚性幹細胞）
FGF：fibroblast growth factor（線維芽細胞増殖因子）
HGF：hepatocyte growth factor（肝細胞増殖因子）
HNF-3β：hepatocyte nuclear factor-3 β（肝細胞核因子3 β）
iPS細胞：induced pluripotent stem cell（人工多能性幹細胞）

In vitro generation of hepatocytes from human stem cells and its application to non-clinical drug development

Yoji Sato[1]/Seiichi Ishida[2]/Kazuhiro Suzuki[1]/Momoko Sunouchi[2]：Division of Cellular and Gene Therapy Products, National Institute of Health Sciences[1]/Division of Pharmacology, National Institute of Health Sciences[2]（国立医薬品食品衛生研究所遺伝子細胞医薬部[1]/国立医薬品食品衛生研究所薬理部[2]）

表1　薬物性肝障害の分類

	中毒性肝障害	特異体質性肝障害	
		アレルギー性	代謝性
用量依存性	あり	なし	なし
動物での再現性	あり	なし	なし
原因	薬物・代謝産物自体の毒性	反応性代謝産物の抗原性 (T細胞依存性肝細胞障害)	薬物代謝関連酵素の個人差 (遺伝的特徴)

肝臓での代謝過程を理解することは，「毒性学」の観点からだけでなく，ヒトにおける薬物の体内動態の評価および複数の薬剤を投与する場合の薬物間相互作用の評価という「薬物動態学」または「臨床薬理学」の観点からも重要である．薬物の肝毒性および代謝過程を非臨床試験のなかで評価する際，ヒト肝細胞・肝組織を用いることで種差の問題の多くを克服することが可能となる．しかし，ヒト肝細胞・肝組織には，入手の難しさ，個体差およびロット差など，大きな問題点が存在している．

近年，幹細胞を分化誘導してさまざまな細胞種を効率的に作製する方法の開発が急速に進んでいる．ヒト幹細胞から肝細胞を効率的に誘導し，肝毒性・代謝研究へ応用できれば，これまでのヒト肝細胞・肝組織を用いた非臨床試験における問題点の多くを解決することができると期待されている．

❶ 薬物性肝障害・薬物応答性

多くの薬物は肝臓で代謝されるため肝障害（肝毒性）を示す可能性がある．薬物性肝障害の肝臓における症状としては，脂肪肝，肝細胞死，毛細胆管性胆汁うっ滞，胆管障害，類洞壁障害，リン脂質症，線維化，硬化，腫瘍などが認められるが，いずれが発生するかは薬物の投与量と頻度，投与期間，および細胞の薬物に対する応答性（薬物動態，薬効・副作用の出方）などによってさまざまである．発症機序をもとにした場合，薬物性肝障害には大きく分けて「中毒性肝障害」と「特異体質性肝障害」とが存在する（**表1**）[1]．

1）中毒性肝障害と特異体質性肝障害

中毒性肝障害の場合は薬物自体またはその代謝産物が肝毒性をもっており，用量依存性であり，動物実験で再現しやすい．したがって，既存の技術でも毒性発現を予測もしくは予防することが論理的には可能である．

これに対し，特異体質性肝障害は薬物に対する特異体質が原因で起きるもので，一般的に用量依存性がなく，動物実験では認められない性格をもち，前もって予測することが困難である．医薬品開発のうえで問題となる薬物性肝障害の多くはこの特異体質性肝障害に属している．特異体質性肝障害は現在ではさらに「アレルギー性特異体質」によるものと「代謝性特異体質」によるものとに分類されている．アレルギー性特異体質性肝障害は薬物の反応性中間代謝産物がハプテンとなり担体タンパク質と結合して抗原性を獲得し，T細胞依存性肝細胞障害により惹起される肝障害である．一方，代謝性特異体質性肝障害は薬物代謝関連酵素の特殊な個人差（遺伝的特徴）に起因する[2]．

2）薬物によって異なる肝障害

中毒性であれ，特異体質性であれ，肝機能障害を惹起しやすいのは化学的に反応性の高い代謝物を生成する薬物であることが知られている．ただし，反応性代謝物を生成しても，ある薬物では惹起される肝障害が中毒性であり，別の薬物では特異体質性となる．薬物によって異なるタイプの肝毒性を引き起こす仕組みは明らかではないが，反応性代謝物が結合する相手のタンパク質種の差による可能性があげられている[1]．いずれにせよ，ヒトにおける反応性代謝物の生成を予測し，その個人差（特に非常に低い比率で存在する遺伝的特徴）と特異体質性肝障害との相関性を評価することは薬物性肝障害の予測において重要である．

3）薬物応答性の個人差

また，肝毒性試験のみならず，薬物動態・薬理試験として肝臓での代謝プロフィールを取得し，薬物の体内動態や複数の薬剤を同時に服用する際にみられる薬物相互作用など，いわゆる「薬物応答性」の個人差を臨床試験開始前に予測することも医薬品開発では重要

表2　非臨床試験においてヒト肝細胞・肝組織を用いる長所・短所

	長　所	短　所
総体として	・医薬品開発における有効性・安全性の予測 ◆ヒト*in vivo*における代謝プロフィールおよび代謝能レベル ◆薬物輸送に関する置換 ◆薬物相互作用の予測	・入手が困難 ・大きい個体差 ・技術要求 ・バイオハザード対応が必要
ヒト肝細胞・肝組織	・代謝プロフィール・代謝能評価可能（第Ⅰ相，第Ⅱ相） ・薬物誘導能検討可能 ・代謝レベルの薬物間相互作用検討可能 ・*in vivo-in vitro* 相関が高い	・入手が困難 ・ロット差が大きい ・高い技術レベルが必要 ・ドナー情報が限定
ヒト肝ミクロソーム	・さまざまな代謝能 ・P450発現が高い ・簡便である ・入手しやすい ・P450レベルでの相互作用検討可能	・多くの第Ⅱ相代謝酵素の欠如により，総体的代謝能評価ができない ・個体差が大きい ・ドナー情報が限定
ヒトES細胞・iPS細胞由来肝細胞（予想）	・代謝プロフィール・代謝能評価可能（第Ⅰ相，第Ⅱ相） ・薬物誘導能検討可能 ・代謝レベルの薬物間相互作用検討可能 ・特定ドナー由来の規格化された品質の細胞を大量に入手可能 ・多くのロットを用意することが可能なので個体差情報と母集団情報の双方を取得可能（iPS細胞）	・培養，分化誘導，肝細胞の分離・回収に高い技術が必要 ・匿名化されておりドナー情報が得られない（ES細胞）

（文献3より）

である．薬物応答性の個人差には，薬物代謝・動態関連分子や薬物標的分子の遺伝的多型，ならびにそれらの発現に影響する環境的要因がかかわっている．したがって，薬物応答性の個人差を予測するためには，これら遺伝的・環境的要因とヒト肝臓または肝細胞・肝組織での代謝プロフィールとの関連を明らかにする必要がある．

2 ヒト肝細胞・肝組織を用いた非臨床試験

安全で有効性の高い新薬を効率的に開発するには，ヒトでの薬効や副作用ならびに薬物相互作用を非臨床試験で高精度・高感度に予測し，早期に臨床試験に入ることが求められる．そのため，医薬品開発の初期段階においては，主に肝毒性・薬物応答性の種差の問題の多くを克服するという意味で，ヒト肝細胞・肝組織を用いた試験の重要性が広く認識されている．肝毒性・薬物応答性予測においてヒト肝細胞・肝組織を利用することの長所・短所を**表2**にあげる．ヒト肝組織は，医薬品候補物質のヒト*in vivo*における代謝プロフィールとそのレベルの予測，肝薬物輸送能，および薬物相互作用予測のための優れた実験系である．また，肝ミクロソーム分画はCYP（シトクロムP450）をはじめとする主要な薬物代謝酵素を含み，取り扱いが簡単であること，凍結試料として入手しやすいなどの利点がある．ただし短所として，ミクロソームには，多くの第Ⅱ相薬物代謝※1酵素群が含まれないことから，薬物全体の代謝プロフィールに関するデータを得ることができない．一方，遊離ヒト肝細胞ならびに初代培養ヒト肝細胞にはすべての薬物代謝関連の酵素が含まれることから，薬物の代謝経路および代謝パターンを明らかにできる．米国食品医薬品局（FDA）が2006年に提示した薬物相互作用に関するドラフトガイダンス[4]のなかでは，新薬の申請書類に初代培養ヒト肝細胞を用いた薬物代謝誘導試験などを資料として添付することが推奨されている．

しかしながら，これら従来のヒト肝細胞・肝組織標本を用いた試験系では，標本のドナーの個人差などに起因するロット差が大きいことが問題とされている．

※1　第Ⅱ相薬物代謝

薬物代謝反応は第Ⅰ相と第Ⅱ相に大別される．官能基形成や開裂反応（酸化・還元・加水分解）である第Ⅰ相反応に対し，第Ⅱ相反応は内因性物質（グルクロン酸・硫酸・グリシンなど）との抱合体化である．第Ⅱ相反応を触媒する酵素は主に細胞質にある．

ロット間のばらつきが大きくてもロット数が十分多ければ試験系として問題はないが，ヒト肝細胞・肝組織標本のもう1つの大きな問題として，わが国における法的制約もあり，その入手が困難なことがある．入手先を海外に大きく依存していることから，人種差の評価が難しく，倫理的に問題を孕むことも問題とされている．特異体質性肝障害の発症率は一般に5,000人に1人未満とされており[5]，例えば多数の特異体質性肝障害発症者の肝細胞を得ることなどは著しく困難である．

特異体質性肝障害のような低頻度で観察される肝毒性や薬物応答性の個人差を十分に予測することが可能な非臨床試験を行うためには，① 用いられるヒト肝細胞・肝組織のロット（ドナー）の数をできるだけ多く，かつ各ロットについては② 規格化された品質（細胞の形質・調製過程）のものを③ 安定的に大量に得ることが求められる．しかし，従来の試験系で用いられるようなヒト肝細胞・肝組織標本ではこの3要件を満たすことは容易ではない．また，可能ならば日本人からの標本を用いることが望まれる．これらの問題を解決する手段として，近年，幹細胞から誘導された肝細胞の利用に期待が集まっている．

❸ 幹細胞からの肝細胞分化誘導

ヒト肝細胞は，たとえ初代培養して増殖させたとしても，徐々に生理機能が減弱し，現在の技術では最長1カ月程度で多くの機能を失ってしまう．また株化された肝細胞由来細胞はごく限られた肝機能しか示さない．胎児の肝臓に存在する肝芽細胞または成体肝臓中に存在するオーバル細胞と呼ばれる細胞は肝幹細胞として肝細胞への分化能をもつが，組織中の細胞数が少ないため，その単離が難しく，非臨床試験に用いることができるほどの体外増殖も困難である．骨髄細胞や臍帯血，羊膜などからも肝細胞様の細胞が誘導されることが報告されているが[6]，肝幹細胞と同様，原材料としての組織・血液の供給量に限りがある．

そこで近年，多能性幹細胞であるヒト胚性幹細胞（ES細胞）やヒト人工多能性幹細胞（iPS細胞）などからヒト肝細胞を誘導しようと試みられている．分化能および自己複製能が有限である体性幹細胞と比較した場合，これらの多能性幹細胞は，ひとたび肝細胞への効率的分化誘導方法が確立すれば，その多能性および無限の自己複製能ゆえに安定した原材料供給が可能となる点で有利である．現時点では肝臓中の肝細胞に比肩するだけの形質をもつ細胞を非臨床試験に用いられるほど大量に人為的に誘導する方法は確立されていないが，ヒトES細胞からの肝細胞様細胞の誘導の効率および生理機能は年々着実に進歩し続けている．ヒトES細胞から肝細胞を誘導する場合，大きく分けて，未分化細胞を内胚葉系に分化させるステップと，内胚葉系細胞を肝細胞へ分化・成熟させるステップとが必要となる．したがって，内胚葉系細胞をいかに効率的に獲得するかが第1の課題となる．

これまでの研究により分化誘導開始時にアクチビンAなどを添加することが内胚葉系細胞への誘導に効果的であることが知られている[6][7]．内胚葉系細胞から肝前駆細胞の誘導にはFGFなどが有効であるとされている．これは，胚発生時に肝前駆細胞を含んだ肝臓前駆組織（肝芽）の出現を誘導する因子の1つがFGFであることと合致する．肝前駆細胞の増殖および成熟にはHGFやオンコスタチンMおよびデキサメタゾンなどが用いられることが多い．

現在，これらの因子の量やタイミングだけでなく新たな液性因子の探索や，転写因子HNF3-βの過剰発現による分化の方向付け，細胞外マトリックス，細胞の足場材料，三次元培養などをさまざまに組合わせた形での培養条件の最適化が精力的に模索されている[8][9]．また，酸素分圧や酸化ストレス状態などの細胞近傍の環境因子，およびES細胞のエピジェネティックな調節などについても最適化の余地があると考えられる．

'07年に初めて報告されたヒトiPS細胞からは，すでに神経細胞，骨細胞，心筋細胞，脂肪細胞，膵臓細胞，血管細胞，造血細胞，内皮細胞など，さまざまな細胞種への分化誘導法が報告されている．ヒトiPS細胞から肝細胞を直接誘導した例はなかなか出なかったが，ごく最近，比較的効率的な肝細胞様細胞の誘導法が報告された[10]．今後の研究の進展が期待される．

❹ 幹細胞由来肝細胞の非臨床試験への応用

ヒトES細胞およびヒトiPS細胞は高い増殖能・多能性・自己複製能を兼ね備えている．これらを再生医

療・細胞治療に応用する場合はがん化の懸念など，安全性上の高いハードルが存在するが，非臨床試験への応用ではその心配がない．そこで，従来のヒト肝細胞・肝組織を用いた非臨床試験の問題点を克服することを目指し，ヒト多能性幹細胞を効率的に肝細胞に誘導する技術の開発を通じて，信頼性が高くハイスループットの化合物スクリーニング系を樹立する試みが現在続けられている．ヒトES細胞およびヒトiPS細胞から肝細胞への分化については現状の技術では効率または形質の面で十分なものとは言えない．しかし，将来的に優れた分化培養方法が確立されれば，一定の品質のヒト肝細胞を安定的かつ大量に供給することが可能となると考えられる．

ただし，受精胚を原材料とするヒトES細胞は倫理的理由などにより多くのドナーからの樹立が困難と予想され，また制度上ドナーを匿名化する必要があるため，表現型と遺伝型との相関の解析が難しいという問題が存在する．一方，ヒトiPS細胞は原材料としての体細胞を多くのドナーから入手しやすく，またドナーの情報も確保しやすいと考えられる．したがって，多数のドナー由来のヒトiPS細胞由来の肝細胞を用いて薬物の代謝プロフィールおよび遺伝子プロフィールなどを取得し，ドナー情報と照合することが可能になれば，肝毒性・薬物応答性の個人差の詳細なメカニズムが明らかにされることが期待できる．また，もし十分な数のドナーに由来するiPS細胞由来肝細胞を得ることが可能ならば，それらを利用してスクリーニング系を構築し，低頻度の特異体質性肝障害および薬物応答性の個人差を予測することが技術的に可能となることも期待できる．

おわりに

ヒト肝細胞・肝組織を用いた医薬品候補化合物の非臨床試験は，今日の創薬において大変重要なものと認識されているが，原材料の入手をはじめ多くの問題が残されている．ヒトES細胞およびヒトiPS細胞からの肝細胞誘導方法を確立すれば，その多くを解決することができると考えられる．特にヒトiPS細胞は異なるドナー由来の多くのロットをバンク化することが可能であり，特異体質性肝障害および薬物応答性の個人差の予測に威力を発揮することが期待される．ただし，そのためには肝細胞誘導方法の確立のみでは十分ではなく，例えば細胞チップ※2のようなハイスループットのアッセイシステムの構築や，*in vivo*における肝毒性・薬剤応答性と*in vitro*の細胞応答性とをつなぐデータベースおよびインフォマティクスなど，周辺技術の開発も非常に重要になる．

※2　細胞チップ

多くの小さな穴（ウェル）をもち，細胞の反応や変化を観察するために細胞をウェルあたり1つずつ均一に入れることのできるチップ．現在，数十万個～百万個のウェルをもったシリコンや樹脂製のチップが製作されている．

文献

1）池田敏彦：日本薬理学雑誌，127：454-459，2006
2）厚生労働省：『重篤副作用疾患別対応マニュアル 薬物性肝障害』，2008
3）簾内桃子，大野泰雄：『摘出ヒト組織・細胞を用いた非臨床研究』（大野泰雄ほか/編），pp125-137，エル・アイ・シー，2005
4）Draft Guidance for Industry：Drug Interaction Studies-Study Design, Data Analysis, and Implications for Dosing and Labeling, U.S. Food and Drug Administration Publication, US FDA, 2006
5）Li, A. P.：Chem. Biol. Interact., 142：7-23, 2002
6）D'Amour, K. A.：Nat. Biotechnol., 23：1534-1541, 2005
7）Hay, D.C.：Proc. Natl. Acad. Sci. USA., 105：12301-12306, 2008
8）Snykers, S. et al.：Stem Cells, 27：577-605, 2009
9）Dalgetty, D. M. et al.：Am. J. Physiol. Gastrointest. Liver Physiol. 297：G241-248, 2009
10）Song, Z. et al.：Cell Res, 19：1233-1242, 2009

＜筆頭著者プロフィール＞

佐藤陽治：国立医薬品食品衛生研究所・遺伝子細胞医薬部・室長（細胞治療薬担当）．博士（薬学）．1995年に東京大学大学院薬学系研究科博士課程修了後，米国シンシナティ大学医学部・ポスドク．'98年に国立医薬品食品衛生研究所代謝生化学部・研究員，2002年に新設の遺伝子細胞医薬部・主任研究官となり，'04年より現職．研究テーマ：幹細胞・体細胞の情報伝達系，再生医療・細胞治療の安全性評価．趣味：登山．

＜つぶやき＞

「『規制科学』という分野に携わっています．一見，威圧感がありますが，実は先端医療の安全性・品質について『何を』『どのように』明らかにすべきかを示すという点で実用化までの電車のレールを敷くような仕事です．」

日薬理誌（*Folia Pharmacol. Jpn.*）**134**，131～136（2009）

Gタンパク質共役型受容体―TRPCチャネルタンパク複合体形成による心肥大シグナル制御

西田　基宏[1]，佐藤　陽治[2]，仲矢　道雄[1]，黒瀬　等[1]

要約：高血圧による圧負荷や虚血などのストレスによって誘発される心筋細胞の肥大化（心肥大）には，細胞内Ca^{2+}濃度上昇によるCa^{2+}シグナリング経路の活性化が重要な役割を果たしている．この過程には，カテコラミンやアンジオテンシン（Ang），エンドセリン（ET）などの神経体液性因子の関与が示唆されており，これらは全てG_qタンパク質と共役する受容体を介して心肥大を誘導する．しかし，G_qタンパク質によるCa^{2+}シグナリング活性化のメカニズムについてはよく分かっていなかった．我々は，ラット新生児の初代培養心筋細胞を用いて，ジアシルグリセロール（DAG）で活性化されるtransient receptor potential canonical（TRPC）チャネル（TRPC3とTRPC6のヘテロ4量体チャネル）がAng II刺激によるCa^{2+}シグナリングの活性化および心肥大形成を仲介することを初めて明らかにした．また，全てのG_qタンパク質共役型受容体刺激が心肥大を引き起こすわけではなく，TRPC3/TRPC6チャネルとタンパク複合体を形成するG_qタンパク質共役型受容体だけが心肥大を起こすこともわかってきた．さらに，TRPC3/TRPC6チャネルを阻害する化合物が個体レベルの心肥大や心機能障害を抑制することも明らかにされてきた．これらの結果は，TRPC3/TRPC6チャネルが心不全治療薬の新たな標的分子となることを示唆している．

1．心不全と心肥大

心不全は，あらゆる心疾患の終末像である．日本国内の慢性心不全患者数は100万人以上と推定されており，高齢化に伴いその数は年々増加傾向にある．心不全患者の5年生存率は50%程度と低い．患者のQOL改善や医療費軽減の観点からも，より画期的な治療法の開発が求められている．

高血圧や心筋梗塞などの負荷が心臓にかかると，心臓は自身を大きく（肥大）することでポンプ機能を維持しようとする．心肥大は，心不全患者にみられる典型的な所見であり，心エコーで容易に，かつ非侵襲的に診断することができる．初期の心肥大は負荷に適応するための代償機構と考えられているものの，負荷が取り除かれないと心肥大は心不全へと進行する．したがって，心不全の前段階で生じる心肥大の抑制が，結果的に心不全の予防・治療につながるだろうと期待されている．

2．病的心肥大とCa^{2+}シグナリング

心肥大は，形態組織学的に，運動や妊娠などで生じる生理的心肥大と，高血圧や虚血により生じる病的心肥大の2つに大きく分けられる（図1）．どちらも負荷によって肥大が誘発されるものの，病的心肥大だけが時間経過とともに心機能の低下（心不全）を起こすことが知られている．病的心肥大の発症・成因には，カテコラミンやAng II，ET-1などの神経体液性因子の関与が強く示唆されている．

病的心肥大の形成には，細胞内Ca^{2+}濃度の増加が極めて重要な役割を果たすと考えられている（図2）．例えば，電位依存性L型Ca^{2+}チャネル，三量体GTP結合タンパク質G_qのαサブユニット，カルモデュリン依存性キナーゼ（CaMKII），カルシニューリンを過剰発現させることで心肥大が惹起される．1998年Molkentinらは，カルシニューリンによって脱リン酸化され活性化される転写因子nuclear factor of activated T cells（NFAT）が心肥大の誘導因子として働くことを初めて明らかにした(1)．NFATは生理的心肥大

キーワード：TRPCチャネル，ジアシルグリセロール，Gタンパク質，受容体，心肥大
[1] 九州大学大学院薬学研究院 薬効安全性学分野（〒812-8582 福岡市東区馬出3-1-1）
E-mail: nishida@phar.kyushu-u.ac.jp
原稿受領日：2009年5月13日，依頼原稿
[2] 国立医薬品食品衛生研究所 遺伝子細胞医薬部（〒158-0098 東京都世田谷区上用賀1-18-1）
Title: Regulation of cardiac hypertrophy by the formation of G protein-coupled receptor−TRPC channel protein complex.
Author: Motohiro Nishida, Yoji Sato, Michio Nakaya, Hitoshi Kurose